ACOUSTIC POWERED MICRO SWIMMER AND ITS BIDIRECTIONAL PROPULSION

by

Ye Zhan

Bachelor of Engineering, Harbin Univ. of Sci. & Tech., 2014

Submitted to the Graduate Faculty of

Swanson School of Engineering in partial fulfillment

of the requirements for the degree of

Master of Science

University of Pittsburgh

2016

UNIVERSITY OF PITTSBURGH

SWANSON SCHOOL OF ENGINEERING

This thesis was presented

by

Ye Zhan

It was defended on

May 12, 2016

and approved by

Sung Kwon Cho, PhD., Associate Professor, Department of Mechanical Engineering and Materials Science

Sangyeop Lee, PhD., Assistant Professor, Department of Mechanical Engineering and Materials Science

Young Jae Chun, PhD., Assistant Professor, Department of Industrial Engineering

Thesis Advisor: Sung Kwon Cho, PhD., Associate Professor, Department of Mechanical Engineering and Materials Science

ACOUSTIC POWERED MICRO SWIMMER AND ITS BIDIRECTIONAL PROPULSION

Ye Zhan, M.S

University of Pittsburgh, 2016

Micro-robots have great potential in biomedical aspects. However, there are no detailed experiments results for micro-swimmer (a micro-channel contains an air bubble inside it) propelling into the human body environment. This thesis describes the micro-swimmer propelling in blood environments, and testing in real blood. Demonstrated through bubble vibration, micro-swimmer can push forward in the blood environment. Meanwhile, I found the phenomenon of the micro-swimmer moving backward in the blood environment. The velocity of stream speed and position of the bubble interface have effect on the micro-swimmer propulsion direction. One the other hand, I find out the micro-swimmer is harder to propel in the blood environment. In order to improve the efficiency of acoustic transmission, I also made the liquid lens to focus sound, which can improve the transfer efficiency of acoustic wave.

TABLE OF CONTENTS

LIST OF FIGURES

1.0 INTRODUCTION

With the development of medical technology, many patients require minimally invasive procedures [1, 2], which can significantly reduce the pain, recovery time after treatment. It can also lower the risk of infection and extenuate the patient during surgery [3-5]. Micro medical-robots can be used in: treatment of cerebral thrombosis and thrombosis in other parts of the body, treatment of cancer and delivery the drug to a specific organ or tissue. Therefore, scientists and engineers hope to invent a kind of robot that can swim in the blood vessels, tissues and organs in human or animal bodies[2, 6-8]. However, those kinds of micro-robots also face many problems[9-11], which are: (1) Energy supply, because the swimming robots mainly work in the human body, it is difficult to design micro- robots into micro size with a small micro-stepper motor and battery propulsion system. Scientists need to design a wireless energy supply to generate kinetic energy. In this way, it can minimize the size and reduce the difficulty of producing. (2) The micro-robots must produce propulsion force suitable for micro-robots controller, because the micro- robots need to adapt to different vessels, it must contend with the pulsating blood flow motion. figure 1 shows the medical tasks for micro-robots.

Tasks of medical micro-robots are shown in figure 1: (1) Micro-robots propel in the blood vessels, which can be used in treating retinal vein occlusion. These kinds of micro-robots can minimize the side effects and improve targeted drug therapies efficiency[12]. (2) Micro-robots can carry the radioactive particles to destroy cancer brachytherapy. (3) A kind of time-varying

magnetic field induction heating miniature robot can be used for treating hyperthermia[13, 14]. (4) Scientists usually conduct stem cell research in vitro, micro-robots can give assistance to apply these results in vivo. (5) Micro-robots can assay tissue samples[15]. (6) Micro-robots can be used as engineering applications to support objects for tissue[16].

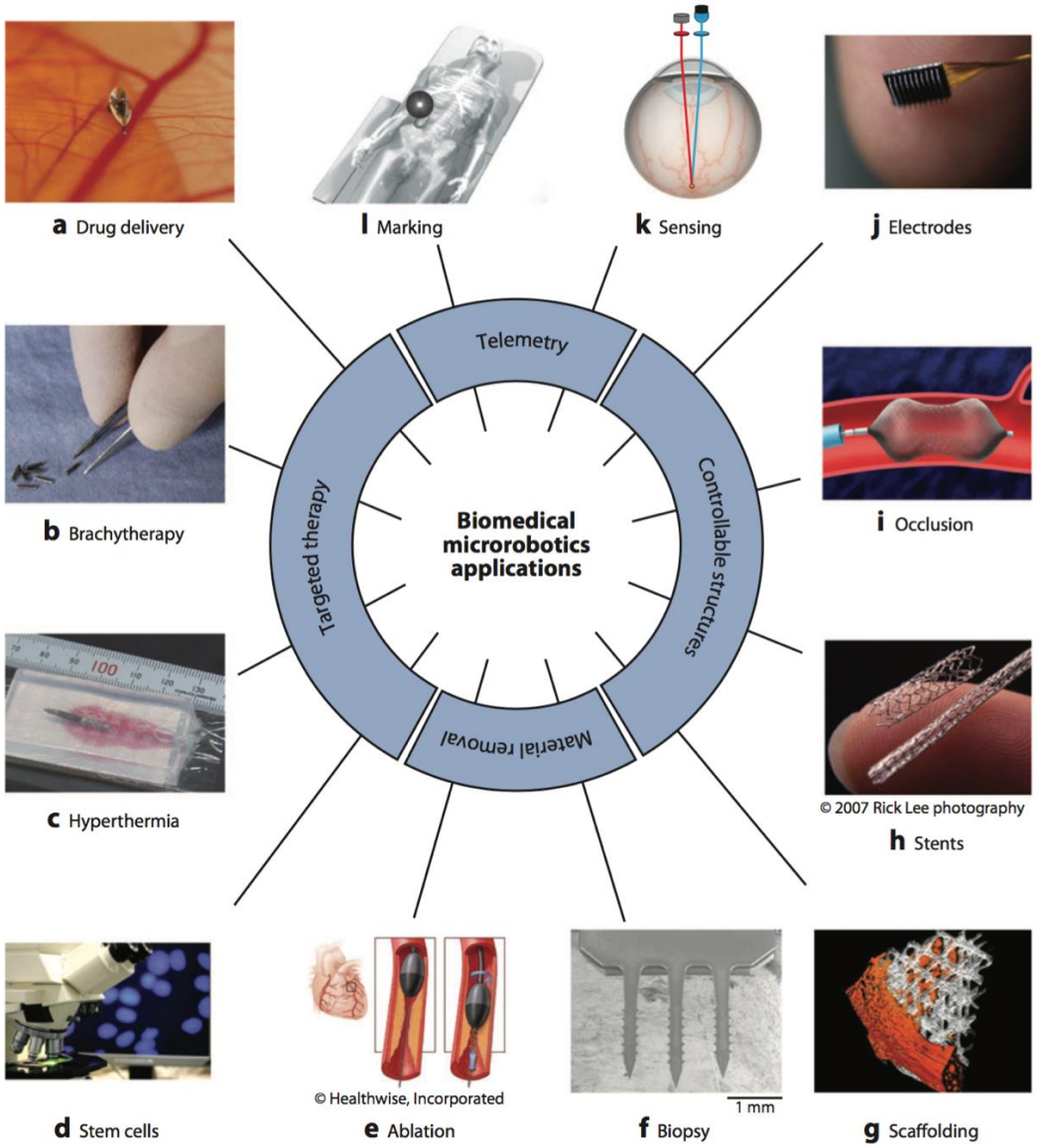

Figure 1. Medical tasks for micro-robots[2]

The principles of promoting micro-size device in liquid is different from in large scale (centimeters, meters) creatures in liquid. Under normal circumstances, biological propel method like human/animal swimming, or mechanical propulsion such as ship move forward, the principles of promoting can mainly be divided into two types: advance by inertia propulsion & viscosity propulsion [17]. In order to discuss this part, we need to study the Navier-Stokes equation (N-S equation). When the Reynolds number is Re, constant density is ρ, liquid viscosity coefficient is η, fluid velocity is V, length has been characterized as L, we can get:

$$\left(\frac{\rho V L}{\eta}\right) = \frac{d\,\vec{V}}{dt} = -\nabla p + \nabla^2 \vec{V} \Rightarrow Re = \frac{\rho V L}{\eta} \tag{1-1}$$

$\vec{V}$ is the velocity vector-field. At low Reynolds number liquid environment, it means stream speed is very slow. For the medical-robot devices, they design in small-scale and working in low-speed fluid environment. The duration time of the action equation (1) is negligible. Fluid flow patterns will not change significantly, and the flow is nearly reversible. Therefore, the results of sliding reciprocation, such as people swimming (go back and forth between the two configurations of body motion) is negligible net movement[18].

Firstly, we should discuss the mechanical motion in the low Reynolds number environment. For volume of micro-robots various from the size of the human body to the millimeter-scale bacteria, propulsion force mainly relying on inertia force. But in the case of liquids having a low Reynolds number[19-23], micro-robots can propel themselves by a way of using a quite different

principle, which includes controlling the direction of movement and the speed of the robots [18]. By using the Navier–Stokes equation (N-S equation) (2),

$$\rho\left(\frac{\partial}{\partial t}+\boldsymbol{\mu}\cdot\nabla\right)\boldsymbol{\mu}=\ -\nabla p+\eta\nabla^2\boldsymbol{u},\quad \nabla\cdot\boldsymbol{u}=0 \tag{1-2}$$

With flow field u and pressure p, we can now solve the force distribution surrounding objects. Moreover, since the incompressible Newtonian fluid density is ρ, we get the stress tensor:

$$\sigma=\ -p\boldsymbol{j}+\eta[\nabla\boldsymbol{u}+(\nabla\boldsymbol{u})^T] \tag{1-3}$$

In the Navier-Stokes equation(2), $\rho\boldsymbol{u}\cdot\nabla\boldsymbol{u}$ is inertia phase, and $\eta\nabla^2\boldsymbol{u}$ is the viscous force per unit volume. In the case of the low Reynolds number, viscous force is dominant.

High Reynolds number conditions are more common for larger creatures, such as fish and humans [24-29]. But for the microscopic world, creatures such as biological sperm swim close to the ovum; by swimming or predation, the paramecium naturally avoid predators. The mechanical principles of swimming are different with biologicals which have large volumes. In the microscopic world, the low Reynolds number is main environmental conditions. Using limbs to swing forward, which is the method that larger creatures mostly used. However, this method is difficult to implement in the microscopic world, because if try to move a fluid by imparting

momentum, after paddling completed, it will be canceled by large viscous damping. So I will discuss how micro-swimmer work in micro & nano-size.

1.1 PROPULSION IN THE MICRON AND NANO-SCALE

1.1.1 Bubble Oscillation

One design of micro-swimmers is: micro-swimmers propel buy bubble oscillation. Propulsive force can be generated by the vibration of air bubbles in the tube [30]. One design of the micro-swimmer is making the tube with one end opened and the other end closed. The teflon tube length is 3mm, the outer diameter is 750 μm and the inner diameter is 250 μm. When device enters into the liquid, since the tube is closed at one end and is filled with a gas, there is an air bubble enclosed within the tube. When given the external sound-field, the bubble will be compressed and vibrated to generate impetus, the liquid will be ejected from the opened end which will generate the propel force. By using MEMS technology, we can produce the smaller tubes[31]. The tubes will be approximately 80×45×530 μm in size. Jian's device is shown in figure 2, it can reach a maximum speed of 45 mm/s. By changing the length of tubes, the resonance frequency of the device will be changed. By fixing the tubes on a plate, the goal of steering and loading the weight can be successful realized. By fixing the tubes with different lengths on the plate, since the different length tube have different resonance frequency, by given different input frequency, the goal of 2-D movement can be realized. As we can see from figure 4. When give input voltage at 370 V, frequency at 5.07 kHz , the longer tube will push the plant move forward. But when we change the input voltage at 210 V, and give frequency at 10.97kHz , the shorter tube will generate main

force to propel the plant move from the other direction, this can help the plate change the movement direction, which will cause the plate travel through the T route.

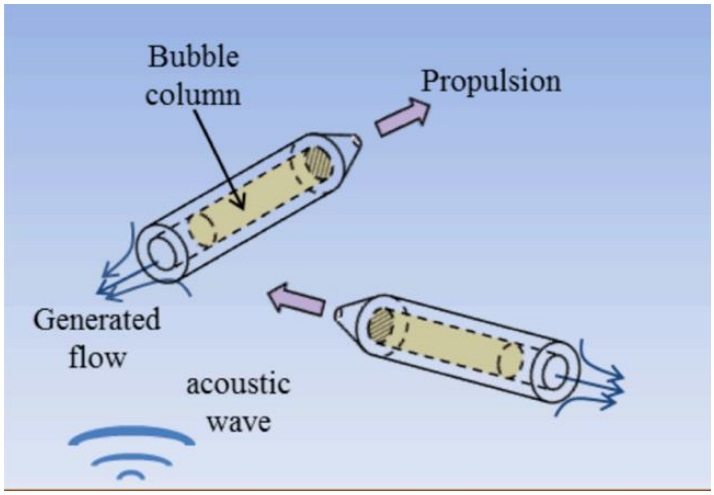

Figure 2. The conception of propulsion by an oscillating bubble column

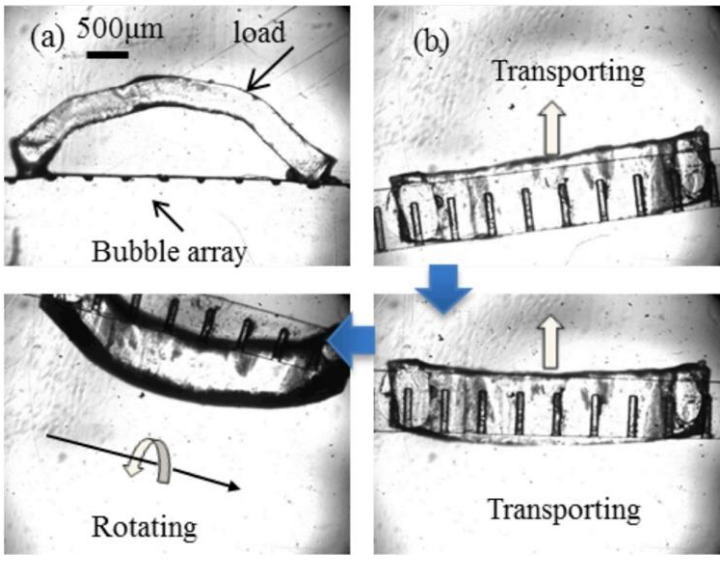

Figure 3. Oscillating bubble-columns attached to a plane and carrying the load

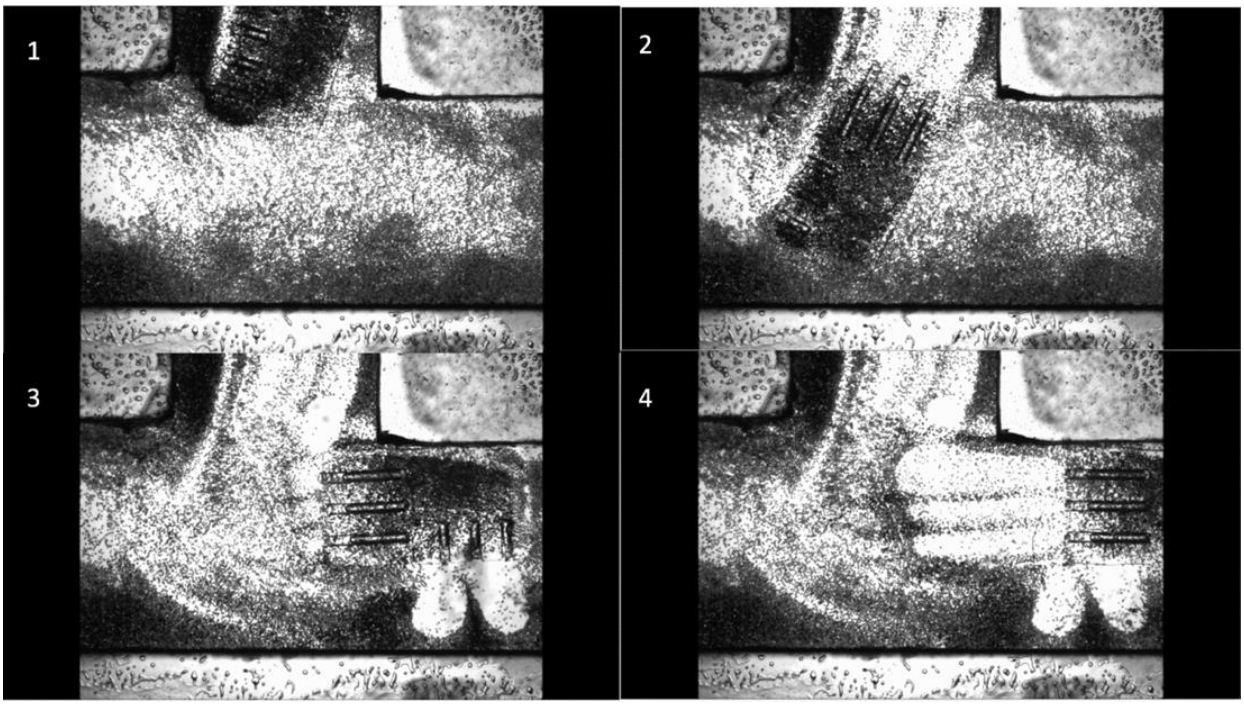

Figure 4. Micro-swimmer 2-D motion

1.1.2 Artificial Cilia/Flagella

Another method for micro-swimmer propel in the liquid with micro size is changing the shape of the micro-swimmers, the limited number of degrees of freedom will result in an irreversible movement. Such a device would need at least two degrees of freedom to make movement [18, 32, 33]. The second kind of design is a swimmer composed by three spheroids, the distance between the spheres change with time and phase [34-38]. J E Avron's group used two spheres with different volumes, which can also cause micro-mechanical motion in the liquid [39].

There are some micro-swimmers propelling at low Reynolds numbers environment using ideal come from bionic. The inspirations of these designs come from the structure of the bacterial flagellum. Such as: synthesis of micron magnetic flagella, which using an external magnetic field to produce torque, it has several interesting designs in papers. These kinds of bacterial cilia bionic

designs mainly can divided into two ideas: one of them is rotating forward to achieve propulsion[40-43]. As shows in the figure 5, (a) shows the structure of a micro-mechanical device: this device relying on a rotating head to drive the the whole device propulsion forward. (b) shows a kind of design: propeller rigidly attached to the micro robot body, so it can rotate itself and generate force from the tail. (c) In this design: flagella spiral wound around micro robot body. The propulsion force also generated by rotated itself. (d) Millimeter-level robot propelling through beef organizations. (e) A design of micron size robot.

The second kind of micro-robot movement mechanical principle is Traveling-Wave Propulsion[44, 45], some micro-swimmers are designed to create a traveling wave to propel themselves. However, the implementation for micro-scale traveling wave propeller is difficult. Imitate for flagella actuation is challenged in manufacturing. Power generation and wireless control also meet problems.

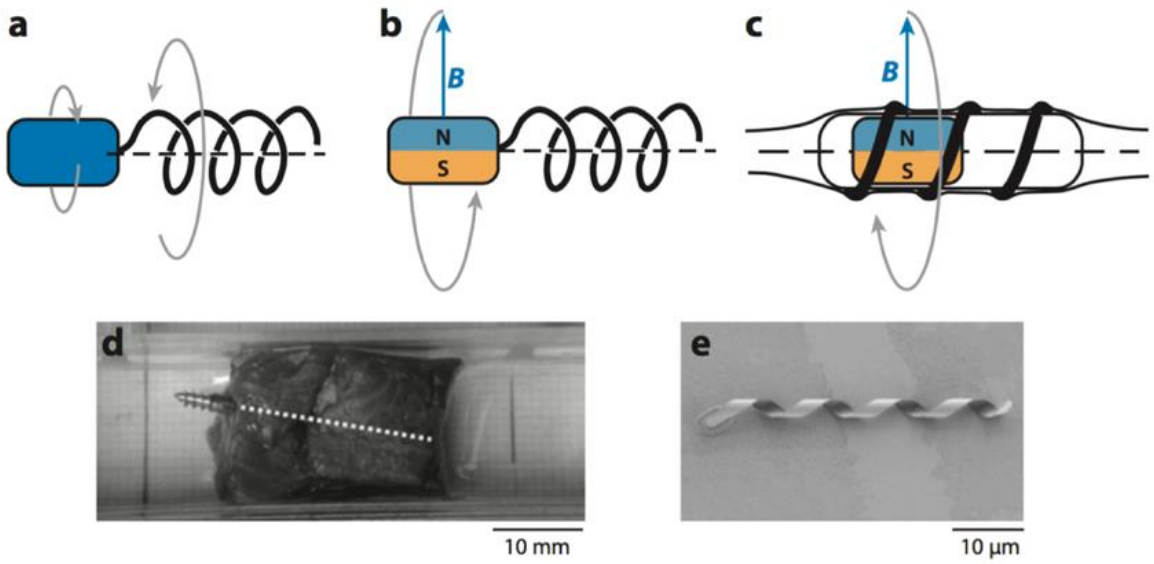

Figure 5. Bacterial cilia bionic design (rotating forward)

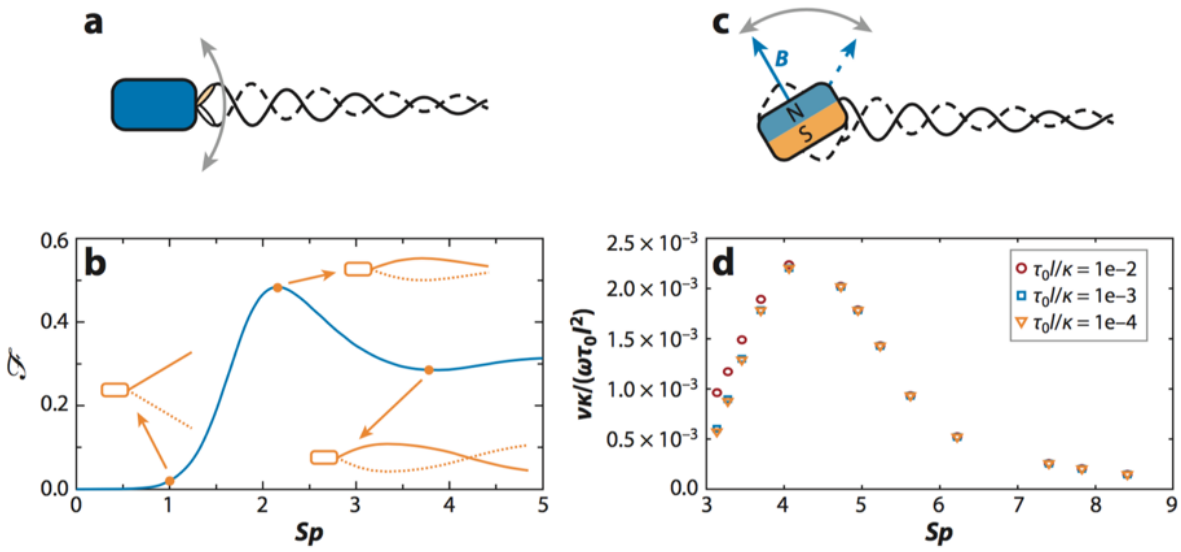

Figure 6. Bacterial cilia bionic design (Traveling-Wave Propulsion)

The figure 6 shows two kinds of propulsions by traveling-wave. (a) A kind of design attached to a miniature robot inside the body vibrator. (b) The figure shows the relationship of *F* vs *SP*, in the figure, *F* is force and *SP* is speed. The elastic tail drive sinusoidal wave. (c) Drive the tail by oscillating magnetic field. (d) The numerical simulation is driven by the head, which is pure sinusoidal wave driven, the relationship of dimensionless torque and speed is displayed in the figure 6.

1.1.3 Driven through chemical energy

The micro-swimmers can also make movement through energy generated by the chemical reaction [46]. As shown in figure 7. Put polystyrene colloid ball into hydrogen peroxide and water solution.

Changing the concentration of hydrogen peroxide can control the movement speed of the ball. Half of sphere adding the platinum which is catalyst for swimming. The reduction of hydrogen peroxide generating oxygen and water, resulting in the directional movement of the sphere.

There is also the other kind of design which is utilize bubble recoiling to make momentum transfer by inertia force propulsion. This is a design using the inertial force motion to propel nano-motor (as show in figure 8) [47].

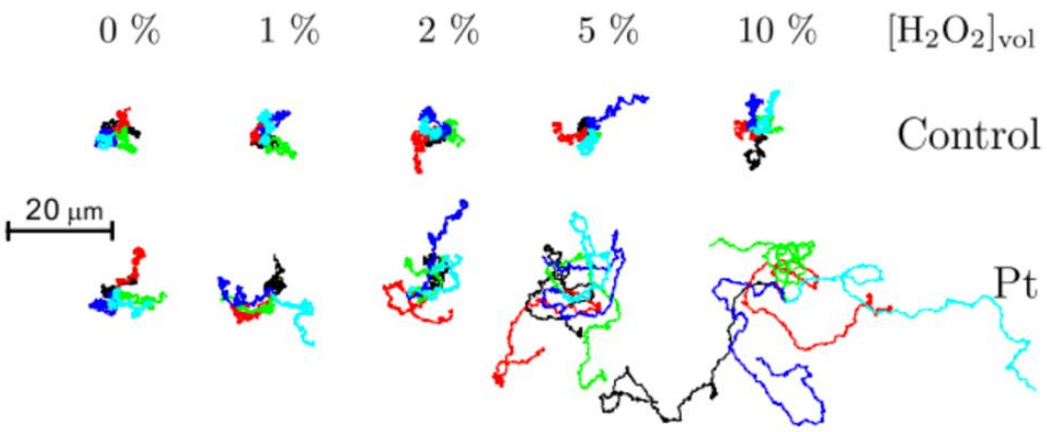

Figure 7. swimmer movement by generate energy through a chemical reaction

The micro-devices can convert chemical energy into kinetic energy. They can make themselves propel forward and rotated[48]. One efficient method is a kind of tube like device to propel itself. The micro-tubules were made by metal thin film [49]. As shown in figure 9, the film is used for the decomposition of hydrogen peroxide, this kind of micro-swimmer using ferromagnetic to control the direction of the magnetic layer.

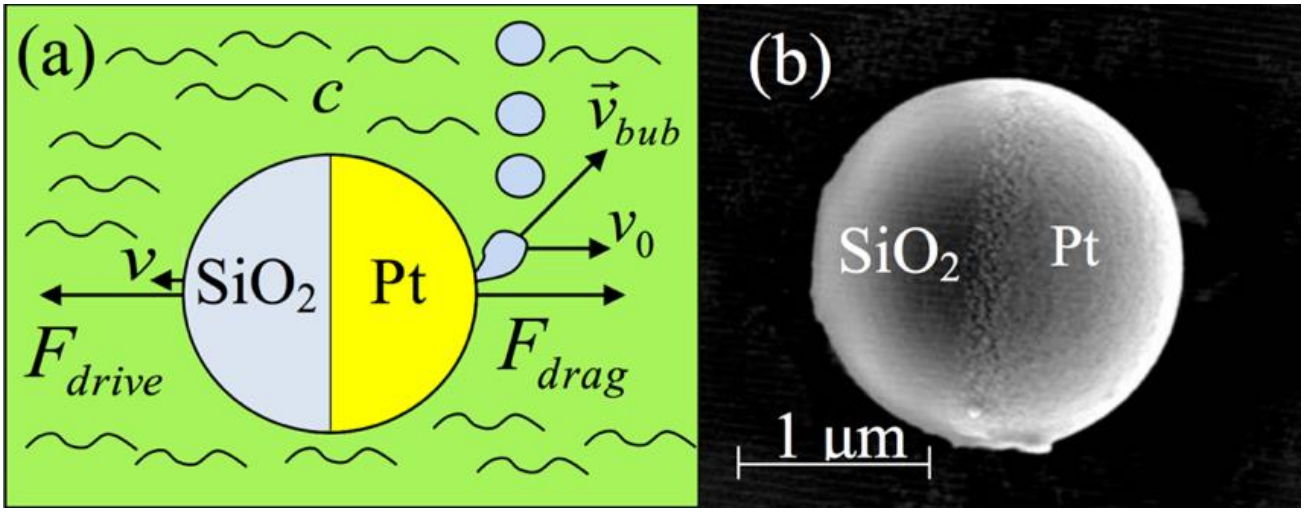

Figure 8. Using of the inertial motion to propulsion nano-motor

At larger opening end, there is a difference between the Laplace pressure, the oxygen bubbles are driven into here. The hydroperoxides are pushed to the smaller openings, which producing a continuous jet stream. Therefore, thrust force is obtained. The maximum speed of this micro-tubule can reach to 2 *mm/s*, which is equal to about 50 body lengths per second.There are also experiment results for tubular polyaniline (PANI) / zinc micro-rockets voluntary movements effective in extreme acidic environment[50].

1.1.4 Brownian motion method

Brownian motion external input signal without biased, the combination of deterministic and stochastic systems can assist in the sub-micron scale particles orienteering [51]. Silica spheres covered by (radius of 2.13 m) half of the gold-coated layer [58].

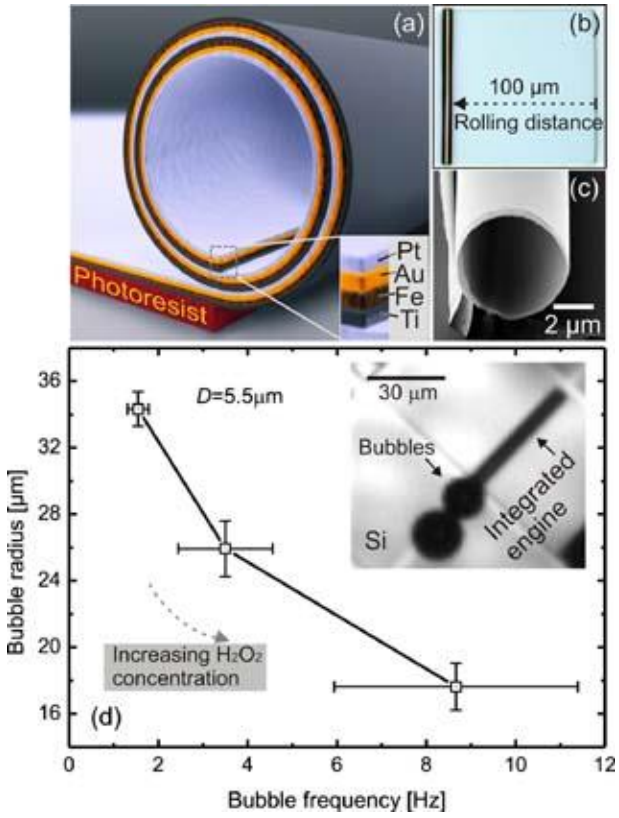

Figure 9. Microtubules structure and testing data

When the light irradiate uniformly, golden coating part will absorb the light, causing the temperature exceeds the critical temperature, which lead to the accumulation of gold-rich cap aqueous phase. Concentration difference will generate thrust force which can push particles. Studies had shown that by changing the green laser beam [52], which is used to produce Janus particles at a temperature difference for direction control. At high light intensity area, particles' moving speeds will up to 0.7 *um/s* as show in figure 10. Self-heating swimming device through solid-self phoretic motion effects, the effects is caused by unbalanced permeate liquid interface, which can also be used to promote the micro-particles [53, 54].So, after understanding the physical principles of how robots working in vivo. I choose the micro-swimmer (bubble oscillation) as

subjects. I will verify the possibility of in vivo work, so I'll put micro-swimmer in vivo environment for testing.

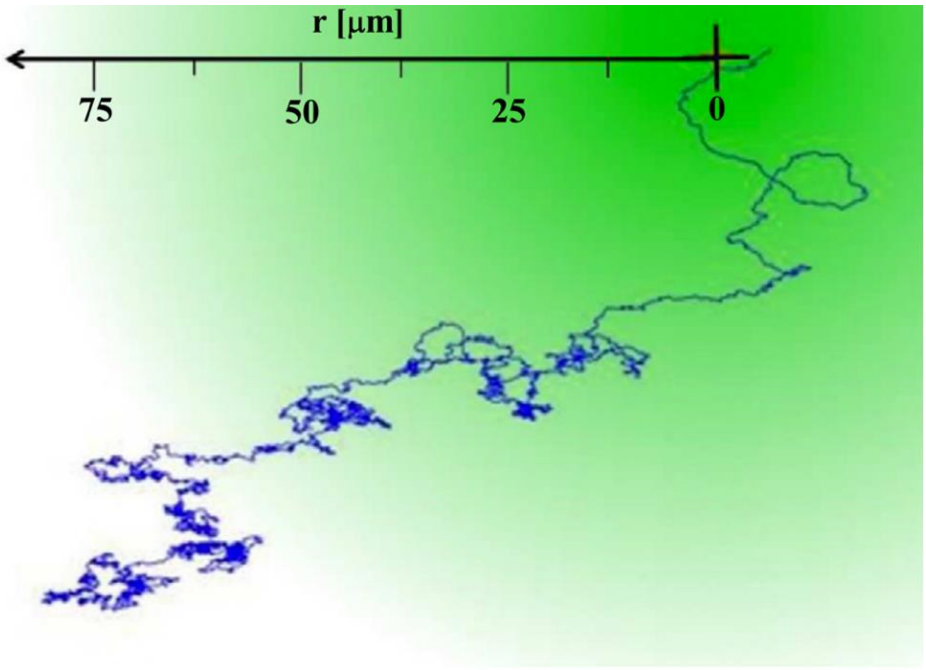

Figure 10. Trajectory of a self-propelled Janus particle by light gradient

1.2 THE AFFECT OF VISCOSITY OF THE LIQUID FOR MICRO-SWIMMER MOTION IN THE FLUID

We know that at the microscopic environment, most of organisms and artificial robots are working at the condition of a low Reynolds numbers, they are propelled using viscous force. By observing

the N-S equation: we can figure out that part of equation: $\eta \nabla^2 u$, which means the viscous force per unit volume. The coefficient of viscosity η will affects propulsion force.

Next, we will discuss different kinds of liquids' impacts on stream flow and fluid field around micro-robots. We chose micro-swimmer made by glass tubes as the test subjects. In previous experiments, the liquid with different viscosities were tested [55-57]. H. C. Brinkman calculated viscous force applied to the micro-particle, which his equation can be used in different viscosity fluids [58]. Using stokes law, the force exerted on the small spherical particles can be calculated, and they got the equation (4):

$$F_d = 6\pi\mu RV \tag{1-4}$$

In this equation: μ is the coefficient of viscosity, R is the particle radius and V is the velocity of the fluid. For the spherical bubbles, there is an equation to calculate resonance frequency of the bubble f_O [59]. In equation (5) a is the diameter of the bubble.

$$af_0 \cong \frac{6m}{s} \tag{1-5}$$

In the case of glass tubes, the equation (6) also given expression in papers [60, 61]. In the equation (6) κ is frequency-dependent parameter determined by the thermodynamic cycle, which is

executed by the gas in the course of the oscillations. P_0 is undisturbed pressure in the bubble, ρ is liquid density, L_B is length of the bubble and L_0 is length of the liquid column comprised between the bubble interface and the exit of the tube.

$$f_0 = \frac{1}{2\pi}\sqrt{\frac{\kappa P_0}{\rho L_0 L_B}} \tag{1-6}$$

Jian Feng given calculation formula through impetus of the bubble vibration, which can descript propel force apply on micro-swimmer (micro-tube)[62]:

$$F \cong 0.8\rho A(af)^2 \tag{1-7}$$

Meanwhile, he also shown the corresponding diagram of relationship between Reynolds numbers and propulsion forces, which is shown in figure 11:

Because the micro-swimmers will eventually be used in vivo as a targeted drug delivery devices or targeted therapy instruments. So biological environment simulation tests are very important. From these equations we can know, the viscosity coefficient of the liquid and the fluid velocity will have large impacts on propulsion force. By review the relevant documents, the density of blood is approximately 1040-1060kg/m^3[63-67]. Compared to the density of water

(1000 kg/m^3). The difference is negligible (4%-6%). However, the coefficient of viscosity of blood is approximately 3.5-4 times of water [68, 69].

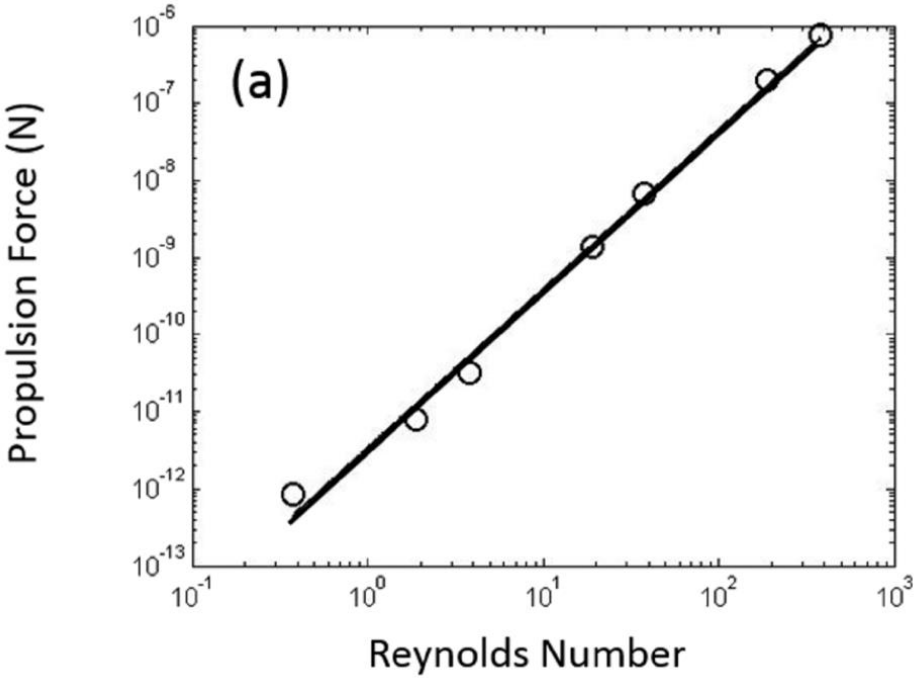

Figure 11. Relationship between Reynolds and propulsion force

Philippe Marmottant & Sascha Hilgenfeldt[70], their study involved in air bubbles deformation and vibration in the liquid. Many treatment methods and biological experiments using the cavitation microstreaming technology [71, 72]. Robin Hui Liu's research [73] mentioned the a kind of mixing liquid flow field by using bubble vibration. However, this paper does not give details of how flow field changed in different liquid environments. S. A. Elder [74] described more details of the flow field of micro-streaming with different liquid viscosity coefficients. In his paper, he gave cases of micro-streaming at a low viscosity coefficient (η=0.01 cm^2/s). The paper showed

the flow fields around the bubble with the increase in bubble vibration amplitude, which we can see figure 12.

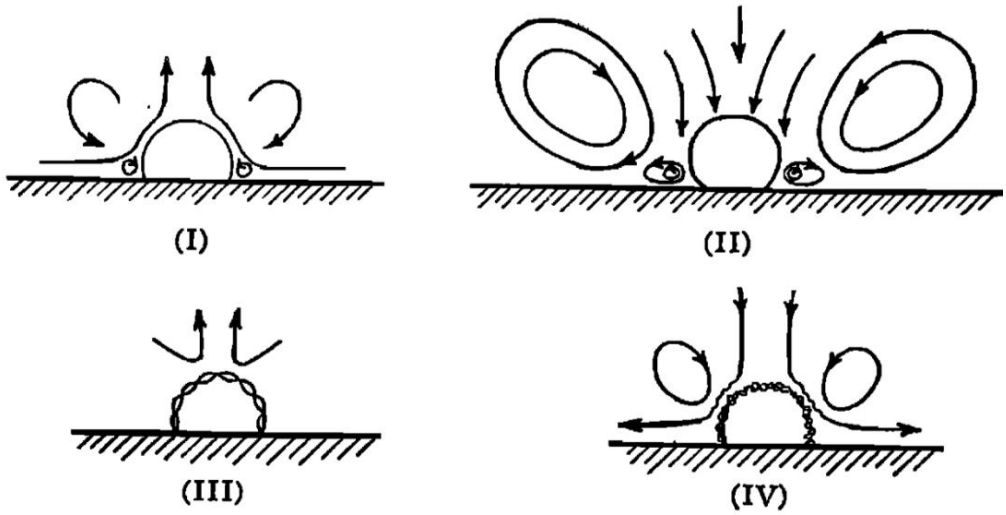

Figure 12. Four different kinds of streaming

However, the author only gave the vibration of circular bubble and the surrounding flow field. But my research will focus on the case of air bubbles vibrate in the tube and find out the details of conditions which will can cause the micro-streaming circular around the open end of the tube.

1.3 LIQUID LENS

In the future research program, we need to apply sound field in vitro to achieve control device in human/animal body. However, we found we mainly use two kind of sound source today, one is point sound source, the other is excitation sound field by vibrating plate. The reasons to use these

two sound sources because sound source structure is simple and easily control. The disadvantage of these two methods are both of these sound source was divergent transmission with low transmission efficiency. Especially when used in blood and human tissue, the energy will get a lot of losses. Such a sound field mode is not conducive to the the device that intend to propel in the human/animal body. In order to improve the transfer efficiency of the sound field, I designed a liquid lens and the focal length can be varied for focusing sound waves.

I was inspired by a video on YouTube upload by Indiana University Physics department [75], In this video, they demonstrated by using of plexiglass lens can focus ultrasound in water. We can see in from video, after using a lens, concentric ripples generated at the focal point is significant enhanced (sound field generated by ultrasonic acoustic transducer at bottom part of the board).

Here is the principle of sound waves through the medium refraction, the acoustic focus and light focus using principles of Snell Law:

$$\frac{sin\theta_1}{sin\theta_2} = \frac{v_1}{v_2} = \frac{n_1}{n_2} \tag{1-8}$$

In equation (8) θ is the angle measured from the normal of the boundary, v is the velocity of acoustic in the medium and *n* is refractive index (unitless) of the medium. Although a solid lens having advantages like simple structure, but it also has shortcomings, for example: a fixed focal length that can not be changed and highly reflective. So I looked up information on a liquid lens. The liquid lens can be used for optical enlarge, various-focal [76-80] and miniature cameras[81].

However, the liquid lens basically using for optical field. There no published results show the experiments of using liquid lens to focus the sound waves. I will make the lens and to verify my ideal: using liquid lens focusing sound waves idea.

The three kinds of liquid lens design are described at following part, we can see them in figure 13.

From figure 13,1. We can see a kind of design to change the focal length of the liquid lens by applying an external voltage [82, 83]. This type of lens having short response time and can continuously change the focus. However, such a lens is typically used for small cases.

From figure 13,2. By injection / pulled out of liquid in chamber to change the curvature of the lens surface of the elastic membrane [76, 84-86]. This type of fluid lens can have various focus length without changing the lens aperture.

From figure 13,3. By changing the boundary of elastic membrane [87]. The liquid within the lens assembly is brought into/out, so the curvature of the film changes, causing the light converging or diverging. A disadvantage of such a lens is not easily kept parallel to the plane of the substrate of the elastic film.

The figure 13 shows the lens types 1,2,3. And 4 is the use of a mechanical structure change the focal length of the lens

Consider the purpose of the experiment is to focus sound wave on the micro-swimmer. The size of the micro-swimmer: diameter is about 600 *um*, length is 1200 *um*. The piezoelectric which generated acoustic pressure diameter is 30mm. So, I chose the second method, such a design can cover a larger area, easily making and does not require application of an external electric field, which is suitable for our experiment case,it can work in various medium, and easily change the focus length.

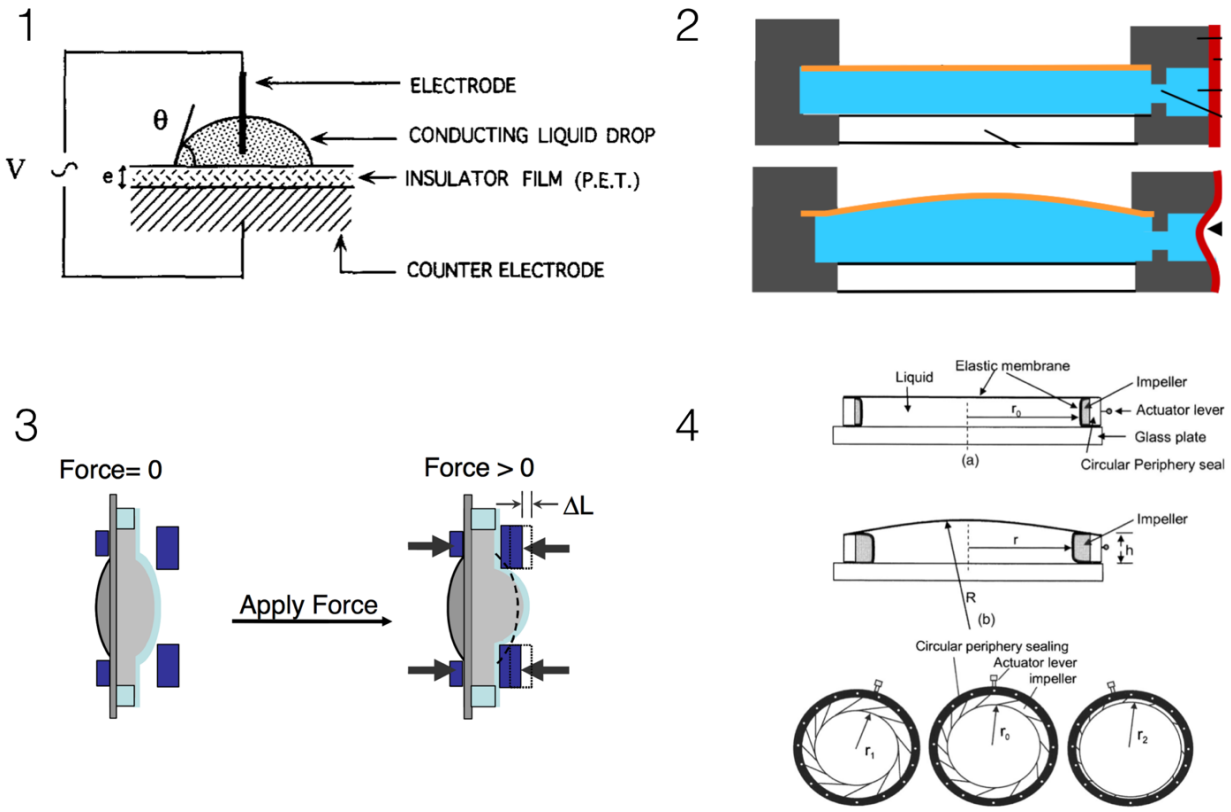

Figure 13. Different types of liquid lens

2.0 EXPERIMENTS

2.1 THE RELATIONSHIP BETWEEN THE VISCOSITY OF THE LIQUID AND THE STREAM SPEED

2.1.1 Experiment of principle

I test with a tube with one end open and the other end closed made by capillary tube, which is based on the experiments results of Jian Feng. I test with this design because its structure is simple and easy to fabricate. One of the important thing is it's do not carry energy source itself. From the experiments results of Jian's work, we know that by arrange several tube together we can carry the load and propel in the fluid environment. So finally it can obtain the goal of drug delivery. On the other hand, by using two different length tube attach on a plant, 2-D movement can be realized. In normal case, Reynold's number can be defined as $Re = \frac{\rho v L}{\mu}$, which ρ is the density of the fluid , v is stream speed, μ is viscosity and L is length of the tube. However, in case of generated by oscillation flow and sound source is extend acoustic wave, which means the propulsion force related to the input frequency, Reynold's number can be re-defined as:

In this equation (2-1), *R* is the radius of the micro-channel, *a* is amplitude of bubble amplitude and *f* is oscillation frequency. We test the tube in high frequency (1.0*kHz*~4.0*kHz*), in this case, we test

in high *Re* number. For the Navier–Stokes equation (2-2): in section of $\rho(\boldsymbol{\mu}\cdot\nabla)\boldsymbol{\mu}$**,** which is a nonlinear term. Assume *V* is one of the solution of the N-S equation, -V may not be a necessarily solution. By time-average the two solution, the result should not be zero, which will cause the movement speed.

$$\mathrm{Re} = \frac{2\rho R(2\pi f)a}{\mu} \tag{2-1}$$

$$\rho\left(\frac{\partial}{\partial t} + \boldsymbol{\mu}\cdot\nabla\right)\boldsymbol{\mu} = -\nabla p + \eta\nabla^2\boldsymbol{u} \tag{2-2}$$

Figure 14. Tube with one end closed and the other end open made by capillary glass tube

Experiments testing glass capillary tubes are closed at one end and open at the other end, as shown in figure 14. Then I would like to explain the production processes which is also shown in figure 15. Firstly, using medical glass capillary tube, which inner diameter is about 300um, and outer diameter is about 600 *um*, cutting it into subsections.

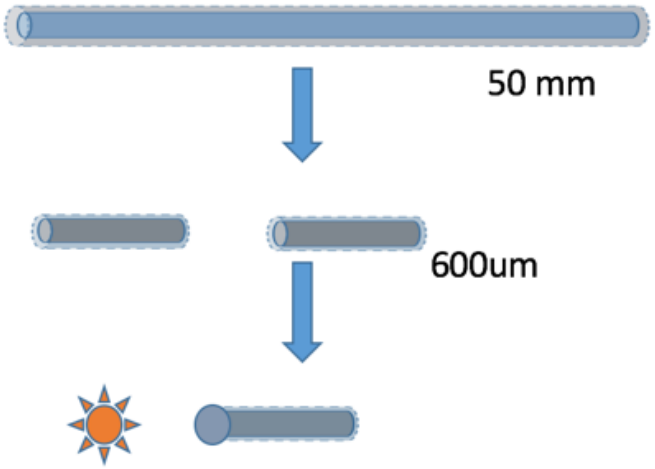

Figure 15. fabrication processes

Each section length is 2500 um ($\pm$50um), one end is heated to melt the glass tube, so I can make it one end closed. Eventually we obtain glass tubes closed at one end open at the other. The propulsion principle is based on the "acoustic scallop"[30]. Which I mentioned above, bubbles trapped into micro-tubes, when the external sound field is applied (frequency is about 2.0*kHz* - 4.0*kHz*), the interface between the gas-liquid bubble periodically oscillate back and forth. Since liquids in and out, the flow field is not a simple symmetry, which means speeds is calculated by mathematical method, and they are not zero, thus micro-tube moving forward.

Navier-Stokes equations have been analyzed and described above: $\eta\nabla^2\boldsymbol{u}$ is the viscous force per unit volume. In the condition of low Reynolds number, viscous forces are dominated.

For experiments of micro-mechanical devices propel in liquids, the "inertial force" also affect smaller, which means "viscous forces" are dominant. So we can get the conclusion: *R*e is a key element of this micro-robot propel in liquids.

Jian Feng's [62] article simulated micro-propulsion streamline under different Reynolds numbers, which is shown in figure 17.

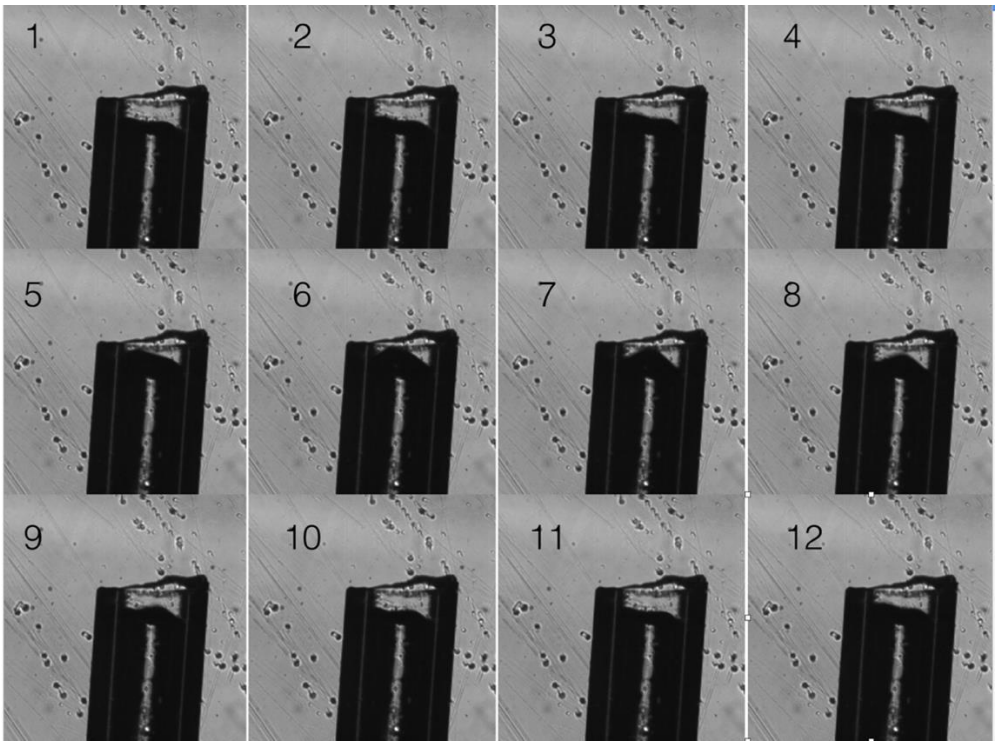

Figure 16. One period of the bubble oscillation

The same amount of fluid inflow and outflow of rate are settled. In the low Reynolds number: *Re=0.38*. We can see from the figure: discharged and enter fluid presents a relatively wide angle, they are almost the same jet flow, except for direction.

Therefore, in this case the fluid flow around micro-device generated momentum almost equal to zero. In high Reynolds number, when *Re = 380*, the input and output liquids are distinctly different, the output flow field showing a straight, centralized state; while in the case of suction, the fluid get together near the opening end of microtubules. Suction at the angle of almost 0-175 degrees, such a huge contrast phenomenon, can generate significant propulsion. Because if we time-average the speed of the fluid flow, the speed should not be zero, and Reynolds number is calculated by the equation: $Re = \frac{2\rho R(2\pi f)a}{\mu}$. In my experiments, I will test the movement of microtubules in different liquids with different viscosities. And these experiments will finally try to prove the micro-swimmer can swim in the blood environment.

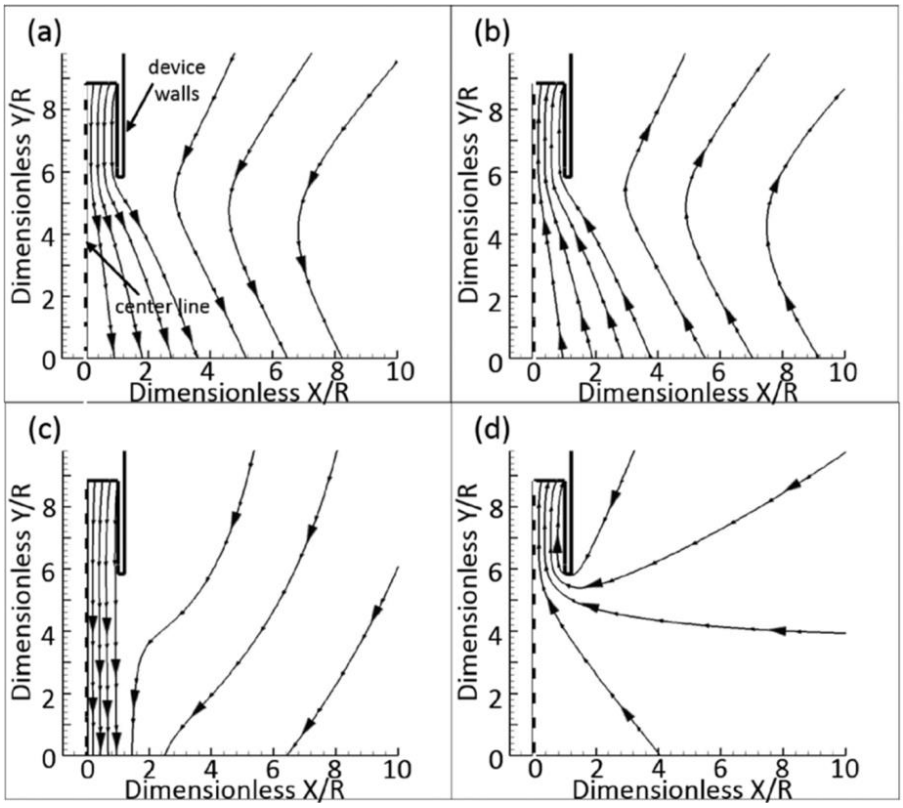

Figure 17. Simulated micro-propulsion streamline

2.1.2 Experimental equipment set up

(1) Liquid choosing

liquids for testing should have the following characteristics: low toxicity, low causticity, easily preserved, viscosity coefficient larger than blood, readily available, inexpensive, and easily to configure different solution viscosity coefficient. Finally, I chose Glycerin (essentialdepot; batch no.892647002536-14132454). The reason for chose the Glycerin are: coefficient of viscosity is much greater than blood (After measure viscosity is [62]1.4Pas; the viscosity of blood is 0.0035-0.004Pas; Distilled water is 0.001Pas). And there is no resistance, which means it can configure a solution in water, and easy to store.

Figure 18. Glycerin

(2) Capillary glass tube selection

I chose the medical glass capillary tube as raw materials, which inner diameter is 300 um ($\pm$25um), outer diameter is 600 um($\pm$25um). As described above, the reason is the glass capillary tubes are inexpensive, durable, easy to store, and not brittle breakable.

(3) Sound source selection

I select the piezoelectric disk (Piezo electric disk transducer 35mm) as sound source. Because the vibration amplitude and frequency of the device can be controlled. The frequency and voltage is generated by the Waveform Generator (Agilent 33220A 20 MHz). The device can produce sine wave from 0 *kHz* to 20*kHz*. For the general case, the resonance frequency of the micro-swimmer is 2.0 *kHz* to 3.5*kHz*, within the scope of the use of equipment. The output current generated by the device, but then through an amplifier (Trek Model Pzd700A High-Voltage Power Amplifier/Piezo Driver) for amplification.

(4) Water tank build up

Water tank was built up by acrylic (Optically Clear Cast Acrylic Sheet, 1/16" Thick, 12" x 12"). After cutting and paste into $50 \times 100 \times 50\ mm$ sink, as show in figure 22. The acrylic pieces pasted on acrylic tank by the chloroform. In order to test piezoelectric locations effects, I attached piezoelectric disks to the different positions of the tank, and I tested its effect to bubble oscillation. Tank and piezoelectric disks are shown in figure 19. The same voltage is applied to the piezoelectric disk, the sound field generated by piezoelectric. By measuring the amplitude of bubble oscillated in the fluid, we can see the different position of the disks indeed have effect on bubble oscillation. When the sound source located at the bottom of the tank, giving the voltage at 49.4*V*, frequency at 1.670 *kHz*, the amplitude of the bubble oscillation is 0.020 *mm*; When the sound source at the top of the tank, given voltage at 50.1 *V*, frequency at 1.670 *kHz*, the amplitude

of the bubbles is 0.017 *mm*. When the given sound source at the side of the tank, given a voltage at 49.81*V*, frequency at 1.670 *kHz*, the amplitude of the bubble oscillation is 0.014 *mm*. I found out that the piezoelectric sheet attached on the top and bottom of the tank, disk will produce the strongest sound field. Attach on the left and right sides of the tank, sound field excitation effect is much weaker.

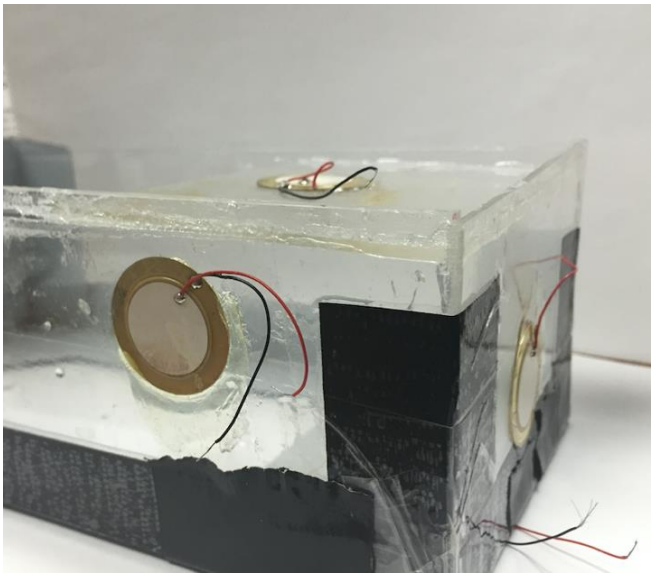

Figure 19. Water tank build up & Piezoelectric in different position

(5) Measuring the viscosity coefficient of the liquid

For the part of liquid viscosity measurement, we use a Rheometer (Anton Paar MCR 52). The measuring steps of this instrument are present as follows: firstly, drip the liquid on the test bench. Meanwhile, on the other end, assembled the sensor with suitable size (with CP-50, CP-25, and other dimensions which can be selected)

The sensor will rotate at a constant speed, and the rotate speed determines the surface shear rate of the liquid, which we dripped it on the platform previously.

Liquid form will tends to the shape of test probe under the squeezed of the sensor. The force applied to the test bench (torque) is measured, which can be converted to shear stress.

(6) High Speed Cameras

I using a high speed camera (Phantom v7.3) to record the movement of microtubules and vibration of the gas-liquid interface.

Generally, I selected recording mode: (1) when recording the movement of microtubules, I choose exposure high speed camera model of: 25 *ISO*, 1000 *fps*, 800×600 *pixel*. (2) when recording the gas-liquid interface vibration & fluid flow at the opening end of micro-tubule, I chose model of: frame is 37000 *fps*, exposure is 25 with 256×256 *pixel*.

(7) Microscope selection

I chose optical microscope when I need to observation micro-tubule movement and and gas-liquid interface oscillation: I chose microscope: Nikon (eclipse te2000-u). I choose different lenses for different cases: (1) CFI Plan Fluor 4x (N.A 0.13;. W.D. 17.1mm; Material No. MRH00040); I use this lens to observe the movement of microtubules. Because I can observe the entire microtubules using lens with this enlarged scale. (2)CFI Plan Fluor 10x: (NA 0.30; WD 16.0mm; DIC Prism : 10x; Material No. MRH00100) I chose a larger magnification lens to observe the gas-liquid interface vibration. I released particles in a fluid, by observing the movement of particles, we obtain the situation of the fluid flow in the liquid at the open end.

(8) Observation of experimental equipment itself microscope selection:

Keyence VHX-600 Digital Optical Microscope (Keyence digital microscope system)

This instrument can meet the measurement requirements such as: (1) measure the length of the tube. (2) Magnification of tube structure. (3) Image is easy to save, and on the other hand, it's easy post-processing the pictures.

2.1.3 Experimental Set Up

Platform set up is shown as figure 20, microscope (Nikon eclipse te2000-u) is connected to a light source. The light source irradiate tank from the bottom. In this way we can observation suspended/immersed tube in the liquid from the bottom of the tank. Since the lens have the limited focus length, I think this is a good solution for both experiments and obsessions. Tank was filled with liquid, put it on the operating stage, the lens is focus at tube. Piezoelectric disk is attached on the bottom and top walls of water tank. As I mention previously, the top and bottom position have the stronger effect, and it also more easily for testing liquid lens which I will discuss later. Piezoelectric ceramic is connected to the amplifier (Trek Model Pzd700A High-Voltage Power Amplifier / Piezo Driver).

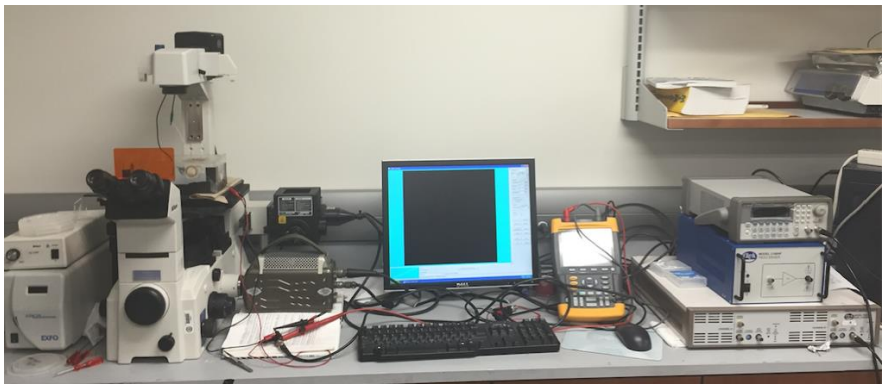

Figure 20. Set up of the experiment

The amplifier is connected to the Waveform Generator (Agilent 33220A 20 MHz), By changing the frequency and voltage inputs, we can find the resonance frequency, and a vibration amplitude for observation. In this way, we can test the bubble oscillation in different input voltage and frequency, which will also help me to research the relationship between the input voltage and bubble position which I will discuss them later in details.

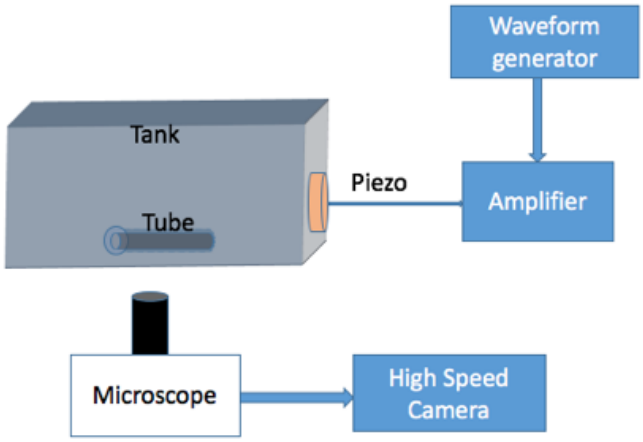

Figure 21. Set up of the experiment

2.1.4 Test Method

The volume of liquid needs to meet the following requirements: (1). Liquid can cover the bottom of water tank and tube can be completely immersed in the liquid. In this case, flow field can be observed in this volume of liquid. (2) In the same volume of blood, the thickness of the blood in the tank can make the light irradiation, and it can be clearly captured by microscope. After testing, I chose liquid volume of 100 *ml* to testing.

In order to formulate an appropriate solution, I calculate viscosity of mixed solution of glycerol and water. These equations come from the paper [88], I also calculation the viscosity

through the data on reference sites and on the web to double check and compare the results[89]. By using rheometer I measured mixed solution of glycerol and water, I can compare the results from experiments and result from equation calculation. I measured water and glycerol mixing solution with ratio 1: 3 (temperature of 25 ° C). From the web, I got the result： 0.00268 $Pa \cdot s$. From the rheometer, I got the result of 0.0027 $Pa \cdot s$, the error between them is 0.7%.

The experiments aim at understand the bubbles oscillation & micro-robot propulsion in liquid with different coefficient of viscosity. And finally proof micro-robot can be propelled in blood. The experimental conditions should be controlled: (1) the same volume of liquid within the tank. (2) The same input voltage and input frequency, which can ensure the vibration amplitudes of the piezoelectric are the same.

Two cases should be considered: (1) Liquids with the different viscosity, bubble vibration oscillation differently. One of reasons might be: bubble is compressed differently, so they have different amplitudes; Another possible reason is: the bubbles are compressed under same conditions with the same amplitude, but effects on the flow field is different. (2) Viscosity and density are different, so reflectivity and attenuation coefficient is also different, in conclusion, acoustic energy transmission capacity is different. So, I will measure into two parts: (1) By applying the same external sound field, measured the fluid flow at the open end of the tube. (2) In the case of the same amplitude, measured tube flow field generated by bubble vibration in different liquid.

Since I can’t measure liquid flow field directly. I tried measure it by using a very fine line, it suspended vertically at the open end of the tube. When the bubble oscillation generates flow field, the fluid flow will give force to the line, causing thin line tilt a certain angle. By measure the angle I can compare details of flow field in different conditions. However, this method has the

following drawbacks: (1) Thin line is very likely to receive the flow field generated by vibration of water tank. (2) Location selection is difficult, because the tube is very small, it is difficult for thin line to stay at the open end of the tube. So I change the method of measure. By placing small particles in solution, the diameter of particles is about 2 *um*, which is shown in figure 22.

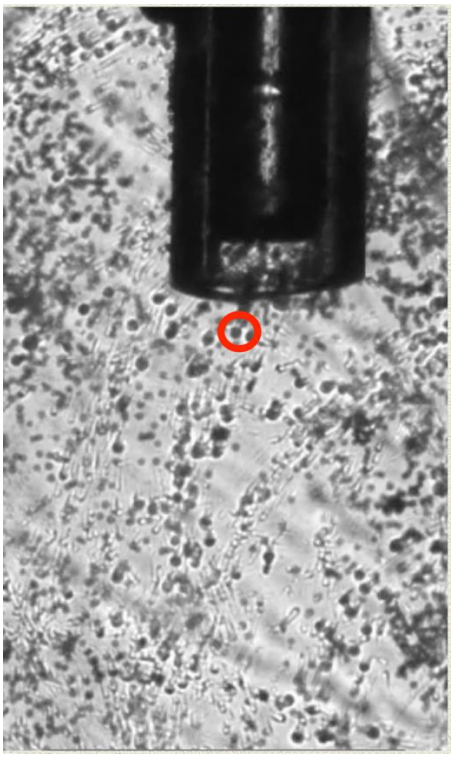

Figure 22. Particles at the open end

Their density is slightly larger than the density of mixed solution, in this way it can smoothly sink to the bottom of the tank. When the flow field generated at one end of the tube, particles will also move with the flow field. High-speed cameras will record every frame of the movement of the particles.

By viewing the high-speed camera photo frame, movement of the particles can be measured. Which is shown in figure 23. And analysis pixel of photo by ImageJ, I can measure particle velocity. Through the particle trajectory-depiction I can grasp the flow field.

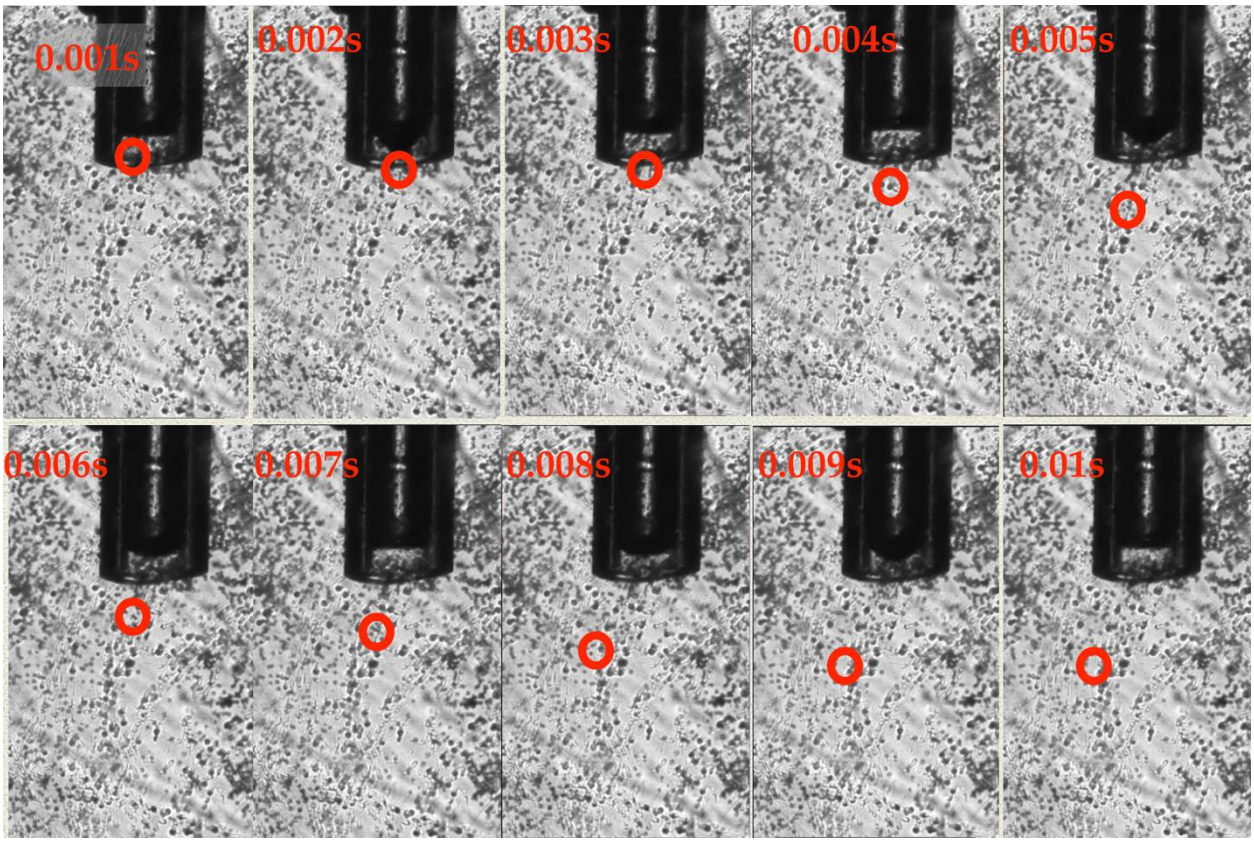

Figure 23. Microstreaming measurement

2.1.5 Experiment results and discussion

In the following part of article, I will present the relationship between viscosity and stream speed, the amplitude of the gas-liquid interface at the open end of the tube and stream speed as well as amplitude of bubble at the open end of the tube and stream speed when applied (same) external sound field. Several things should be noted that, in this test, I used tubes which length is 600~1200 *um*, outer diameter is 600 *um*, inner diameter is 300 *um* made by medical glass capillary tube. Gas-

liquid interface is below the open end, and depth is about 150 *um* (±20 *um*). With applied voltage at 75*V*, frequency at 3.7 *kHz*. Experimental results of relationship between viscosity coefficient and stream speed are shown in figure 23.

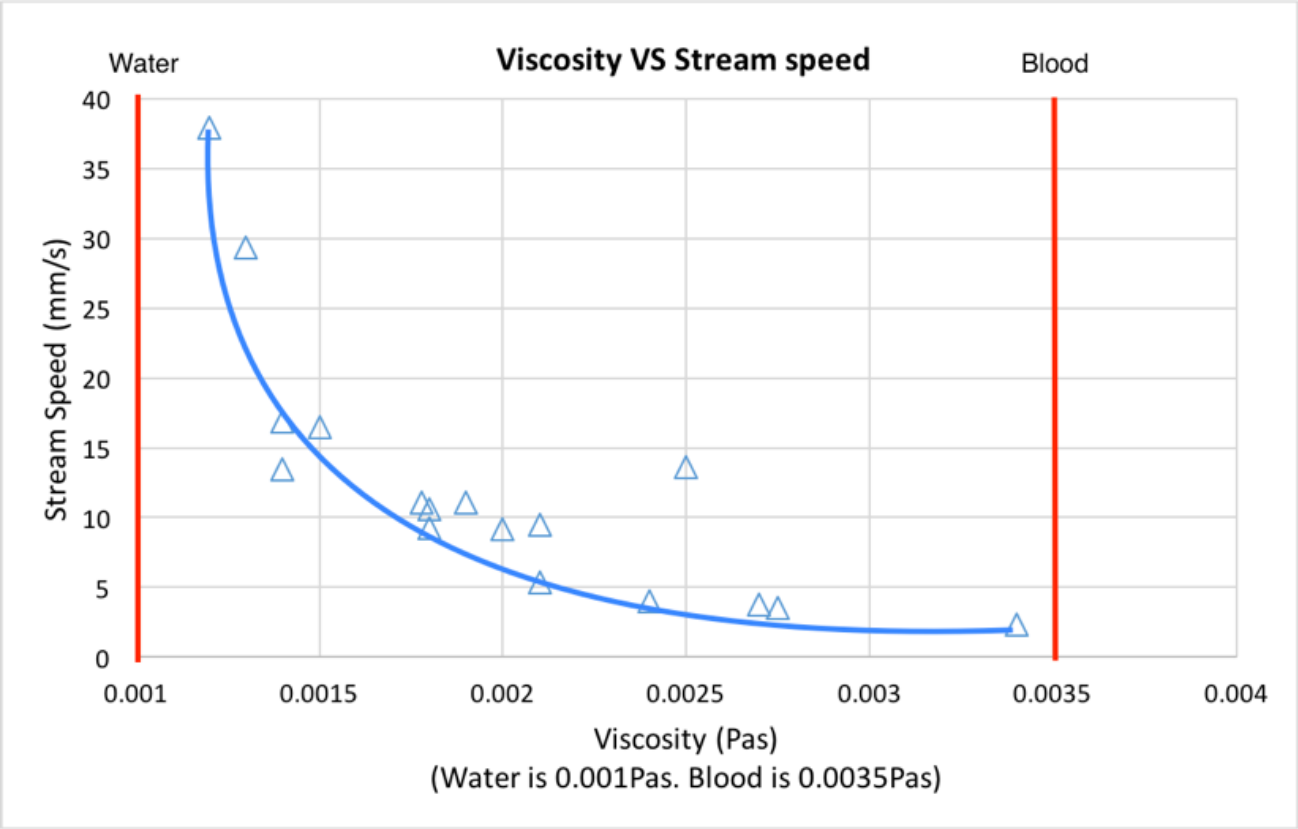

Figure 24. The relationship between viscosity coefficient and stream speed

From the chart, we can see under the same external experimental conditions, with the increasing of viscosity, the stream speed become slower. I expound several explanations: (1) With the increasing viscosity, the amplitude of the bubble becomes smaller, so as the stream speed. The amplitude of the bubble oscillation has a large effect on stream speed, because oscillation

amplitude determines the initial velocity of the stream speed, it means with the large bubble oscillation amplitude, the initial speed of the particle become larger. (2) In the case of high viscosity liquid, particles oscillate back and forth, this can cause the particles move forward slowly because when give time average of the the velocity, back and forth can lead to low average speed. I chose use High-speed Camera shooting with 10000 *fps* frames to record a period of one tube vibrations. Figure 25 shows the overall status of the tube. figure 26 is an amplification for the black box in figure 25.

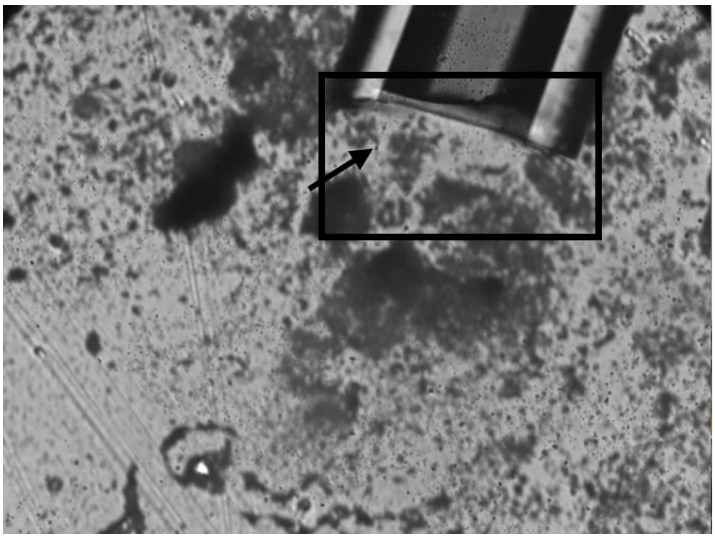

Figure 25. Whole view of the tube oscillate in high viscosity

So, I show the movement of micro-particles in a continuous period of time at the open end of the tube.

From the figure 26 we can see that the particles in the opening paragraph oscillate back and forth, so there is no obviously push forward.

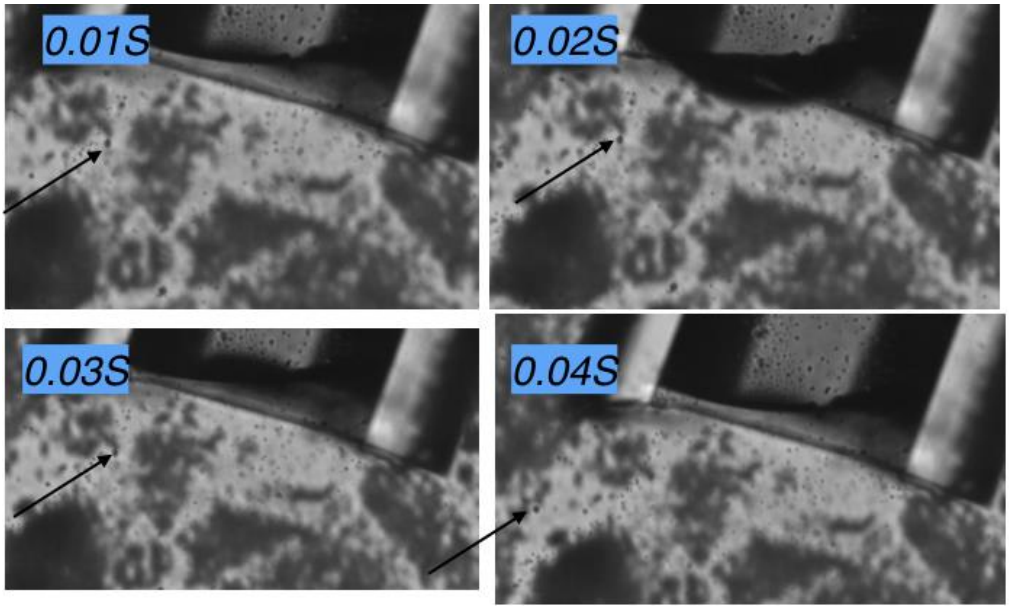

Figure 26. View of micro-particles oscillation

(3) Physical properties of the liquid are different with different viscosity coefficient: such as density and speed of sound, although the same sound field is applied to tube, with different attenuation coefficients, stream speed might be different. From the equation of characteristic impedance, we can see:

$$z = \rho c \tag{2-3}$$

Which z is characteristic impedance, ρ is fluid density and c is sound speed. For the first explanation, I did the following experiment to proof it. The results can be found in figure 27. The figure 27 shows that with the increase in viscosity, the amplitude of the bubble oscillation indeed

reduced. To further verify my idea, I measured the relationship between the oscillation amplitude of the bubble and stream speed. We can see in figure 28 that with increases of the oscillation amplitude, the stream speed is also increased, which is directly proportional to each other.

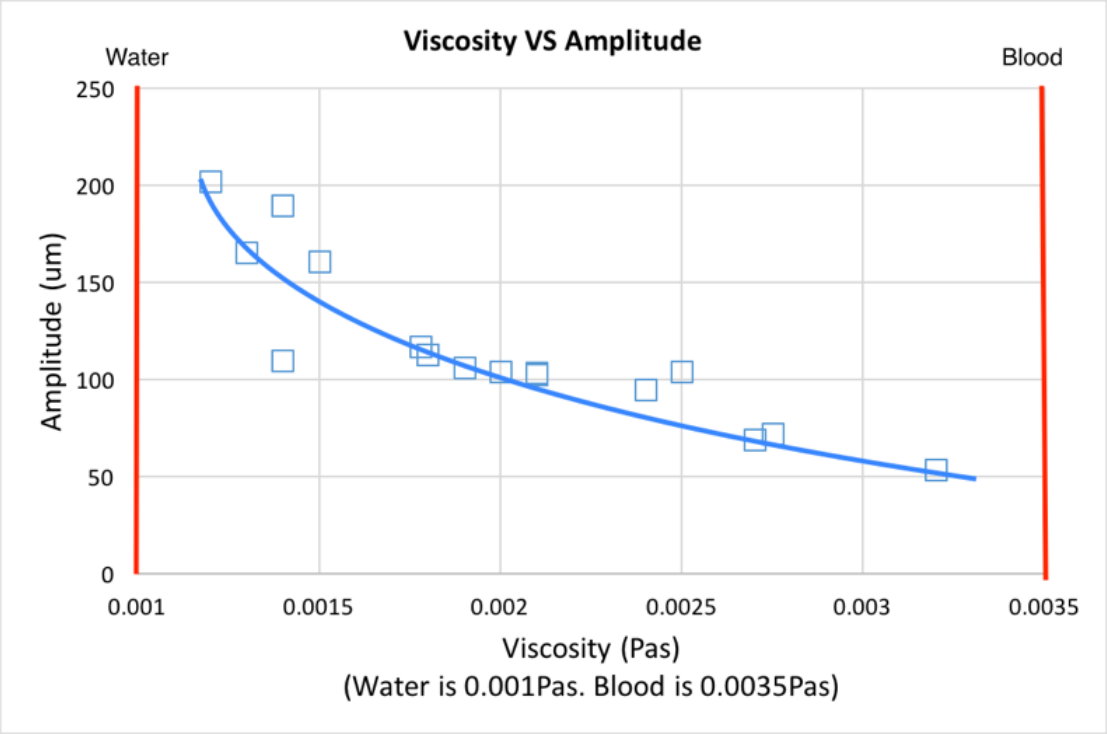

Figure 27. The relationship between viscosity and amplitude

So we can get to the conclusion that, when given the same external conditions, the higher the viscosity is, the slower stream speed is. Because the amplitude of the bubble will lower at the high viscosity solution, which will cause the initial velocity of the fluid stream speed lower. The reason for small bubble oscillation amplitude is in high viscosity solution, by checking the document, I found out that the density of the liquid and sound transfer speed also larger than low

viscosity liquid, which leading the attenuation coefficient is larger, causing the energy transfer efficiency is very low. On the other hand, from these data we can predict that it's more difficult to propel the micro-swimmer swim in the blood environment than water.

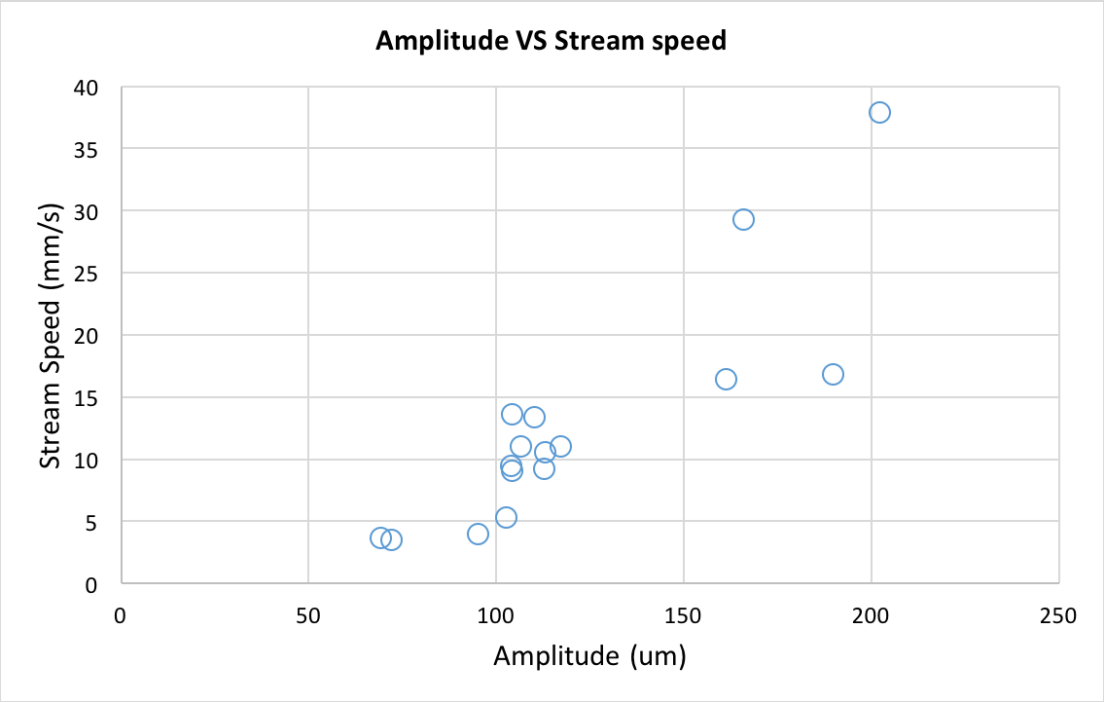

Figure 28. The relationship between amplitude and stream speed

If micro-swimmer working into the actual blood environment, due to physical properties changes, causing the low efficiency of acoustic transmission, and will directly affect the oscillation amplitude of the bubble. Thus the micro-swimmer propulsion in the blood may be move slowly, causing actual application more difficult.

At the same time, I also measured the relationship between the viscosity coefficient and the input vibration frequency, I measured the velocity of the fluid flow field at the tail of micro-

robot. By simulating the liquid viscosity coefficient as same as blood. By changing the input frequency, we can observe the relationship of stream speed of fluid and input frequency variation.

Figure 28 show with the change of frequency, stream speed changes. We can see from the figure 28, with the input frequency changes, there are several resonant frequency peaks appear. There are peaks at the frequency of 3.2 *kHz*, 3.9 *kHz*, 4.3 *kHz*, 4.9 *kHz*…

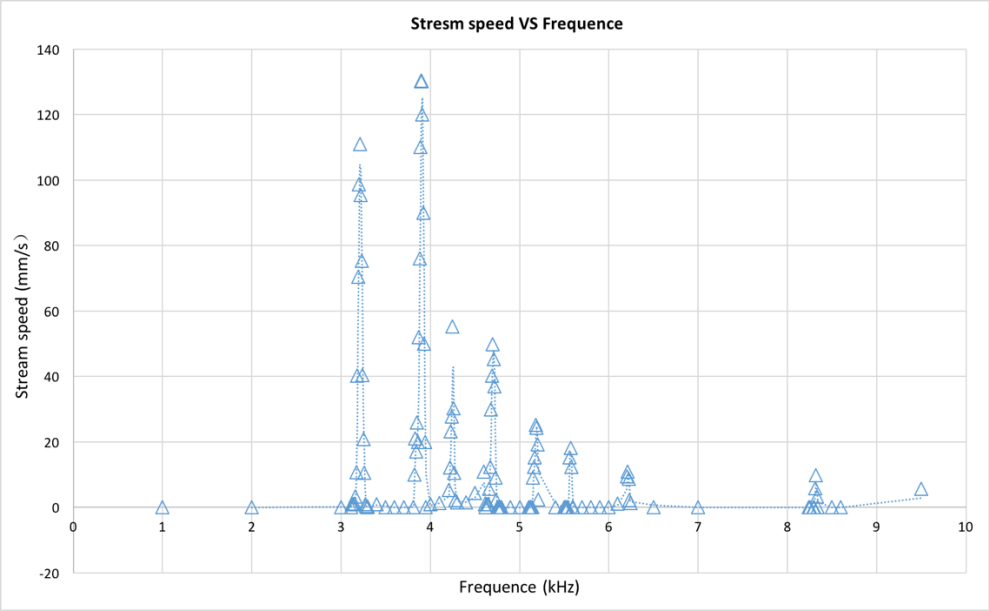

Figure 29. The relationship of input frequency and stream speed

Then, I tested frequency various from 2.0*kHz*~3.5*kHz* with two liquids with different viscosities. We can see from figure 29, "single resonance range" of water is significantly larger than the " single resonating space" of solution of mix of water and glycerol. By calculating their Q factor we know that the Q factor of water and glycerol solution is obviously a lot smaller than Q factor of water. We can also see the bandwidth of water and glycerol solution is wider than the

band width of water. Except the effects of different physical properties of the two liquids, I think one of the reasons is water is much easily to propel by oscillation of bubble than mixed solution of glycerol. The Q factor is calculate by the equation $Q = \frac{f}{\Delta f}$, where f is resonance frequency. And Δf is bandwidth.

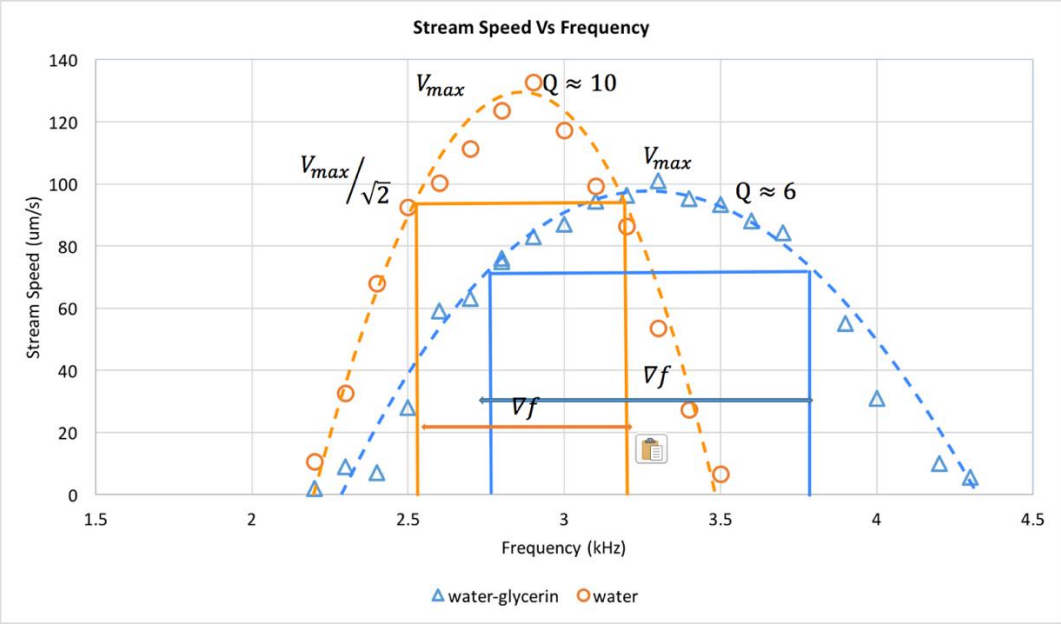

Figure 30. The relationship between stream speed and frequency (water / water-glycerin)

2.2 TUBE PROPULSION IN THE BLOOD

2.2.1 Experiment Principle

The experimental principles are as same as previous experiments. I use the capillary glass tubes which closed at one end are immersed in the blood, so there will be a bubble of blood enclosed in

a glass tube. When applied to externally of the sound field, bubbles will oscillation because of the external sound field, the bubbles can be compressed elastically then oscillate back and forth. By changing the flow field, the driving force will also be changed in the open produced by bubble at the end of the glass capillary tube. One thing should be mentioned that the physical properties of the water and the blood is quite different, which means the blood has different density and viscosity with water. Moreover, since blood component red blood cells, platelets, so the blood is non-Newtonian fluid. Before the implementation of this experiment, it is difficult to determine whether can we push the device forward through the oscillate of bubbles. From the previously experiment we expected that micro-swimmer is harder to propel at large viscosity environment.

2.2.2 Experimental result

Experimental platform set up is same as previous one. Experiment was divided into two parts. (1) Micro-robot propel testing in plasma. (2) The micro-robot propelling testing in blood.

Because the blood is dark color liquid with high viscosity, and the microscope lens is viewed from bottom to the top. I test different volume of blood to make sure the clarity of observation. Finally, I chose 100 *ml*. I choose 100 *ml* because micro- robot can be completely immersed in the water tanks liquid with this volume, and microscope can easily catch the observation target in bright light.

Tests in plasma: the density of plasma is about 1025 kg/m^3 [90]. By actual tests for viscosity at 0.00226 $Pa \cdot s$. The results are shown in figure 31 below:

Because plasma easily observed under the microscope (it's a kind of light color liquid compare with whole blood), which we can see a clear micro- swimmer forward movement. One

thing should be noticed that here we can also clearly see the flow field at the open end of the tube (shadow of lines in the figure 31).

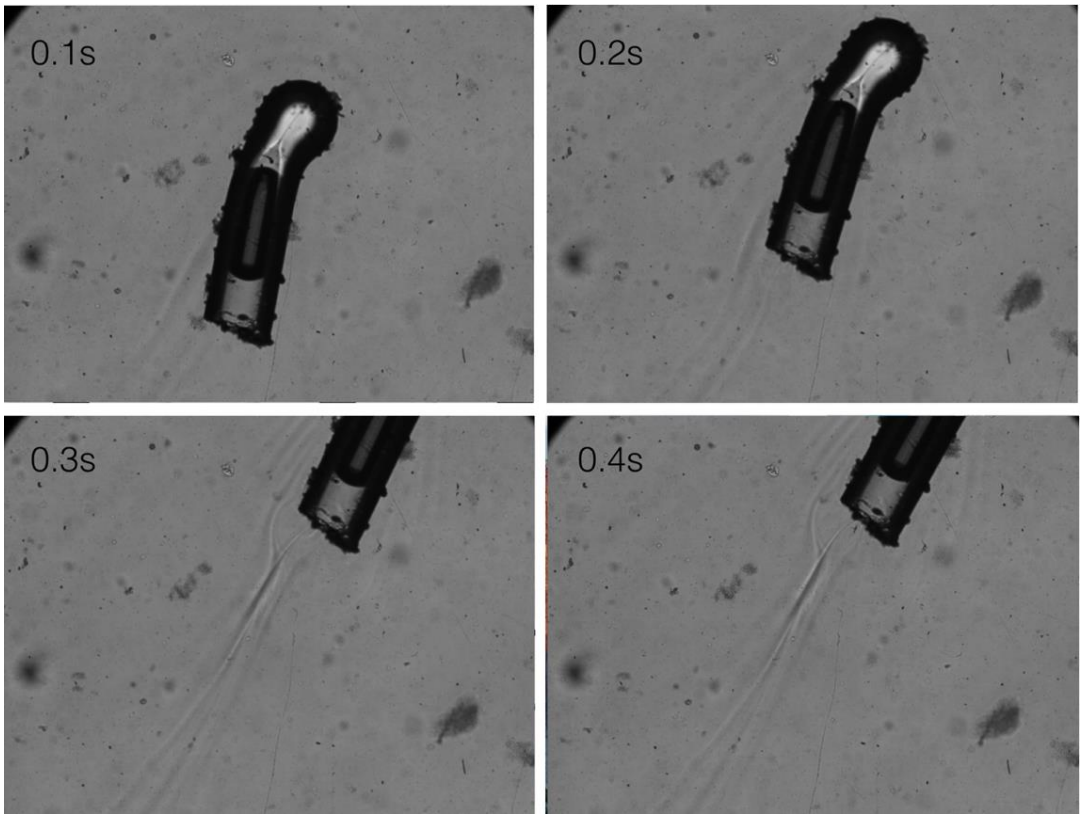

Figure 31. Testing for micro-swimmer in plasma

By vibrating bubbles, tail of tube produced a backward propulsion flow field (can be seen from the shadow of the tail tube). And in this experiment the gas-liquid interface is within the open end of the tube. The strong and powerful results show that perhaps micro- swimmer can move forward in the blood. Then I did micro-robot experiments in the blood, which can be seen in figure 32.

The average density of whole blood for a human is 1060 kg/m^3[91]， By measuring the viscosity of blood by rheometers I know the viscosity of blood is 0.0036 $Pa \cdot s$. This a slightly different compare with document provides. This different may caused by anticoagulant in blood, but the error is within an acceptable range.

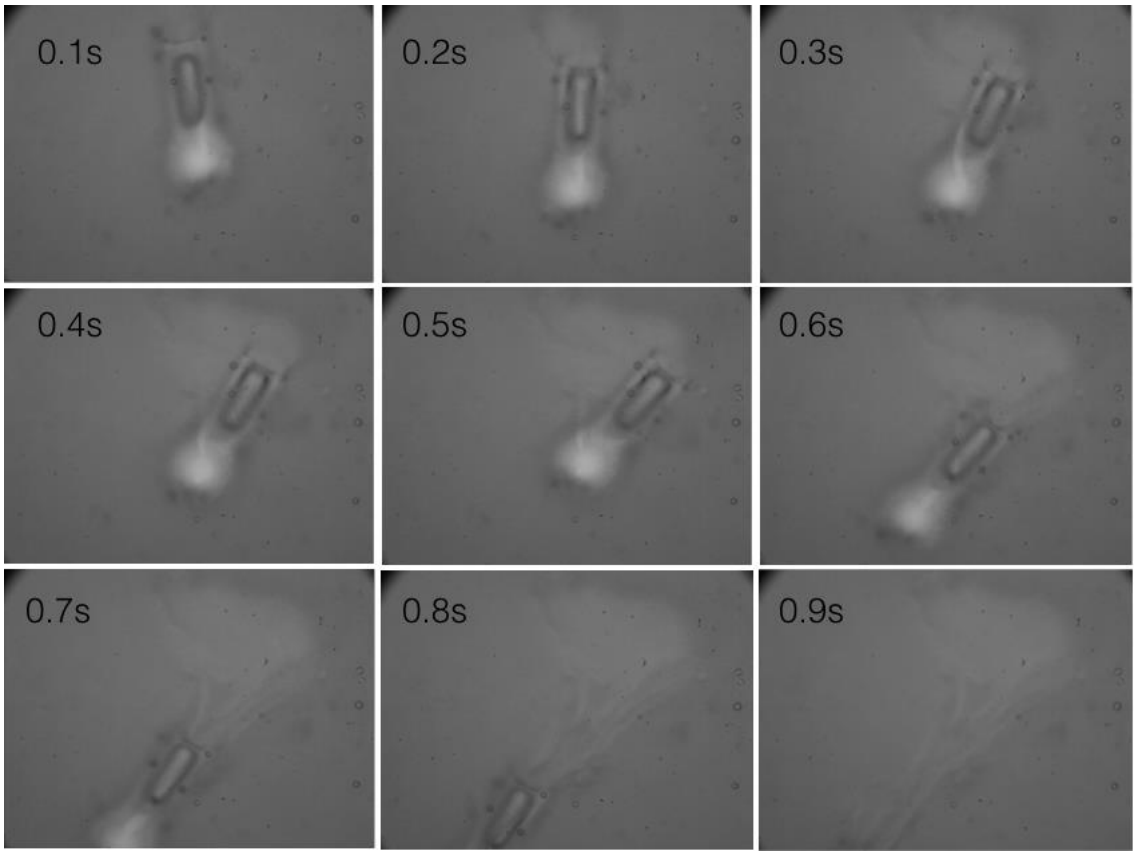

Figure 32. Testing micro-robot movement in blood

From the comparison of the two figures, we can see that in the plasma micro-robot moving speed is significantly faster than that in the blood, and blood viscosity coefficient is larger than plasma. So this also to verify the correctness of the above simulation experiments.

2.3 EFFECT OF THE GAS-LIQUID INTERFACE POSITION TO MICRO-SWIMMER

2.3.1 Experiment principle

During the experiment I found a “unusual” phenomenon: the position of the bubble in the tube may exist in different positions. Typically, when given external sound field a period of time. The bubble itself growth in the liquid and bubbles will show the trend of growing out (In different liquids, the bubble growth with different speed. In lower viscosity liquid bubble growth is faster, liquid with higher viscosity was growth slower according to the experimental observation). The different position of the bubble will affect the micro-swimmers propulsion. During the experiments I have observed the phenomenon that tube can move backwards. I find this phenomenon in blood environment firstly, then I repeat the experiments results in in water, water-glycerine environment, I can also observe the same phenomenon.

2.3.2 Experimental equipment building up and testing method

The experimental equipment set up is same as the equipment that measure relationship between the viscosity coefficient and stream speed.

The method used in the experiment will be described below: short-term external sound field is applied causing bubbles maintain in different positions. When gas-liquid interface stability, I given different external sound field causing different stream speed, then I observe the relationship of the different positions to micro-swimmer propulsion. I calculate the time-average speed of the micro-swimmer and compare the data. The reason for using time-average speed is there are a lot

of factors that may effect the instantaneous velocity. Such as the smoothness of the bottom of the tank. By measure the average speed can reduce the error.

2.3.3 Experiment Result and discussion

Three tube with different length (length between 600~900um) were tested under the same external conditions. The results were shown in figure 33. When the gas-liquid interface within the open end of the tube, only two backward movement result show in experiment 2 (I definition stream speed negative for the reverse movement is backward movement), the other are all forward movement. When the gas-liquid interface above the open end of the tube, there are a large number of backward movements were observed. It can be seen from the experimental data. In case when gas-liquid interface above the open end of the tube at the stream speed of 50 *mm/s* to 100 *mm/s*. (In the chart, positive / negative represented direction, so here I just want to show the size of the speed so I ignore the sign of direction). Tube will move backward. When stream speed is 100-250 mm/s tube will move forward.

Here, there are three factors that may affect the results of the experiments. The viscosity coefficient of the liquid; the position of the bubble interface and stream speed of flow field. First of all, I tested the effect of the different viscosity on stream speed in different bubble position cases, the experimental results are shown in the figure 34. I tested three different liquid viscosities. In test results we can see, when the gas-liquid interface above the open end of the tube, liquids with different viscosities were at different stream speeds, there are data of both the forward movement and backward motion.

It is impossible to determine whether the viscosity is the decided the move direction of the micro-robot. For the case of the gas-liquid interface below the open end of the tube, we can see

that with the increase in the viscosity the reverse movement greatly reduced. So may be a position of the bubble and the oscillation amplitude will influence the direction of movement.

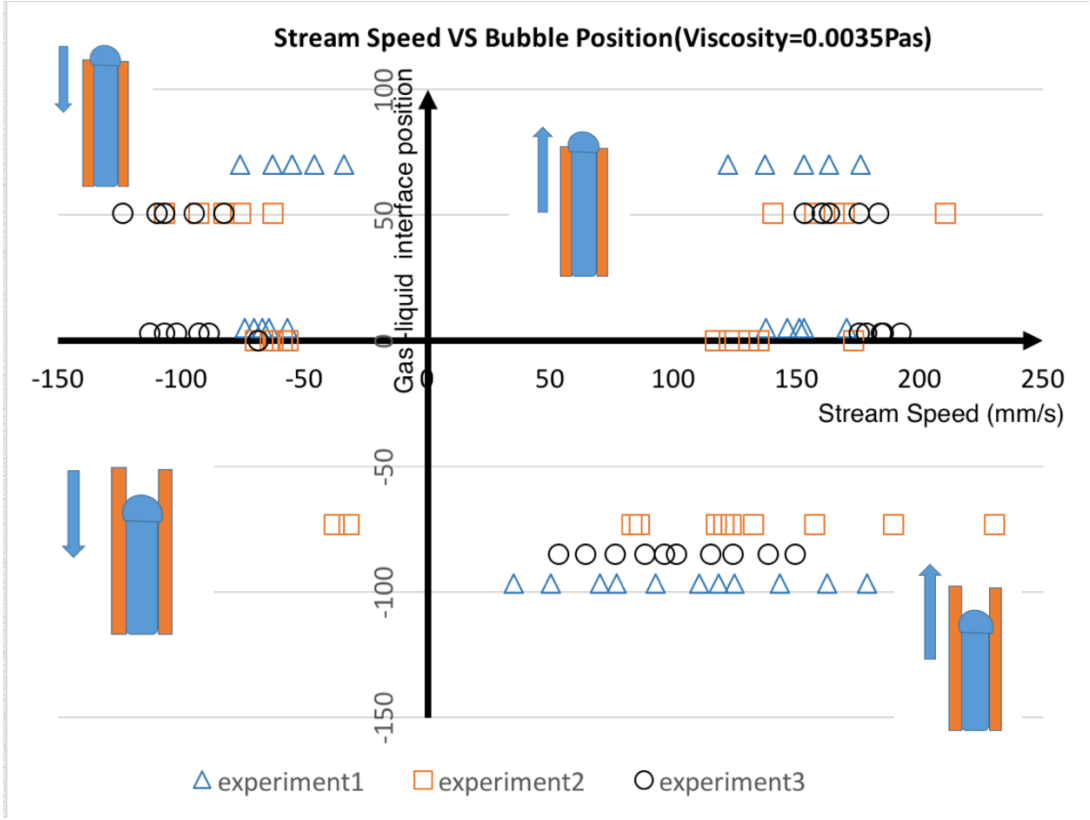

Figure 33. The relationship between stream speed and bubble position

In order to proof my idea, I prepare two liquids with different viscosities, they were tested by applied different external voltage, I obtain different external sound field. The experiment results are shown in figure 34 and figure 35.

We can see when the viscosity is 0.0035 $Pa \cdot s$ and the gas-liquid interface within the open end of the tube, During the test, there is no case of backward movement appears. However, when

gas-liquid interface above the open end of the tube and stream speed at low speed, the device has a backward movement phenomenon. One thing should be notice that at the large stream speed, ($\geq$ 30mm/s) the device trend forward movement.

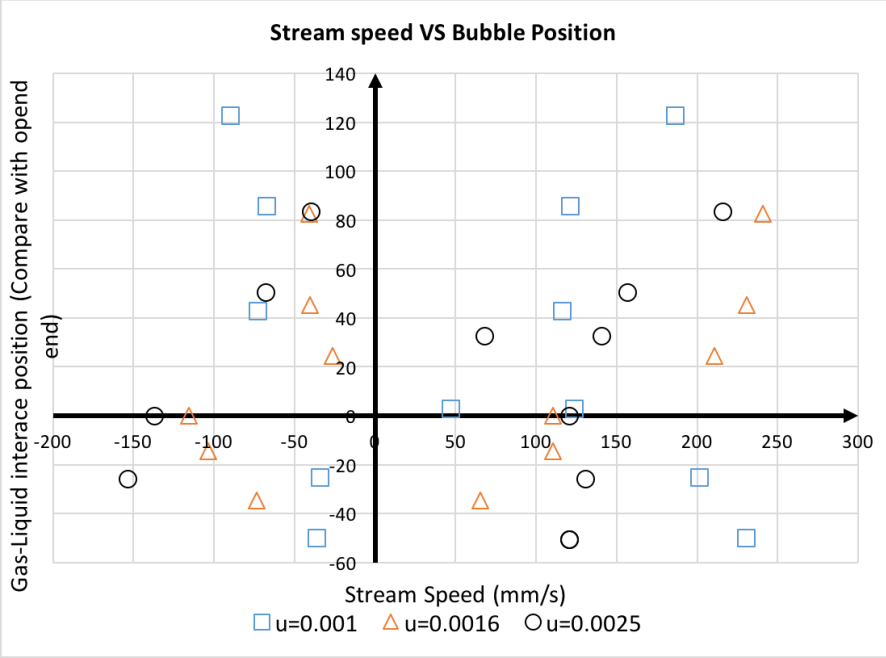

Figure 34. The relationship between stream speed and viscosity

In water (u = 0.001 $Pa \cdot s$), equipment movement trend to be the same. But one thing different is the backward movement phenomenon also appears, under the conditions of stream speed is large enough and the gas-liquid interface within the open end. I think when applied the large externally sound field the large bubble oscillation amplitude is generated. At that time, the gas-liquid interface at the peak of period was outside in the open end. This is the similar situation when gas-liquid interface outside the open end.

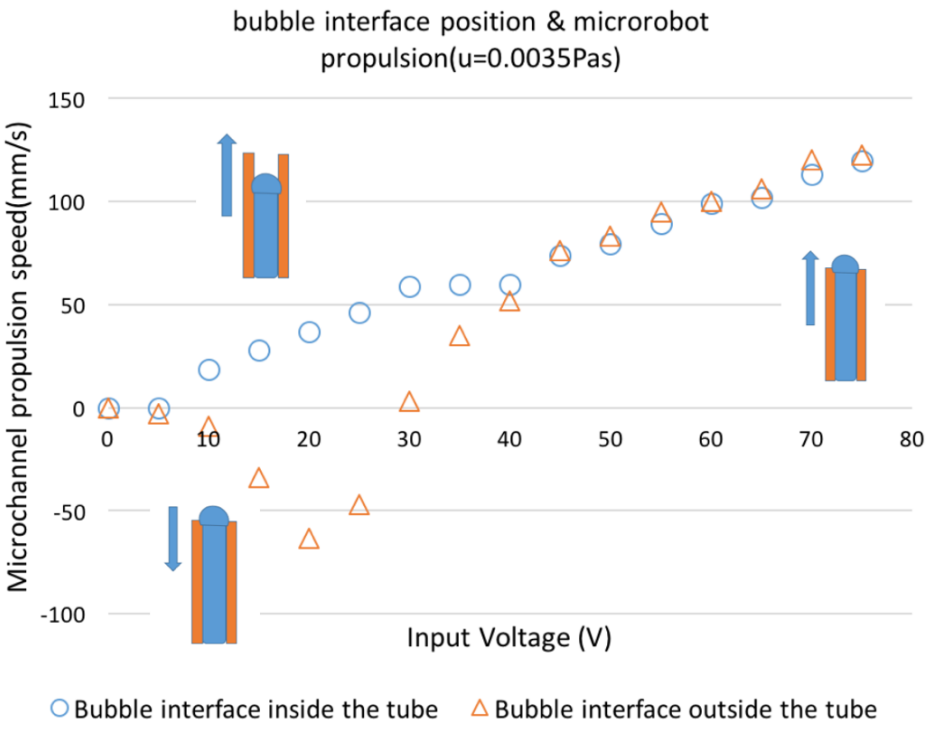

Figure 35. The relationship between stream speed and input voltage

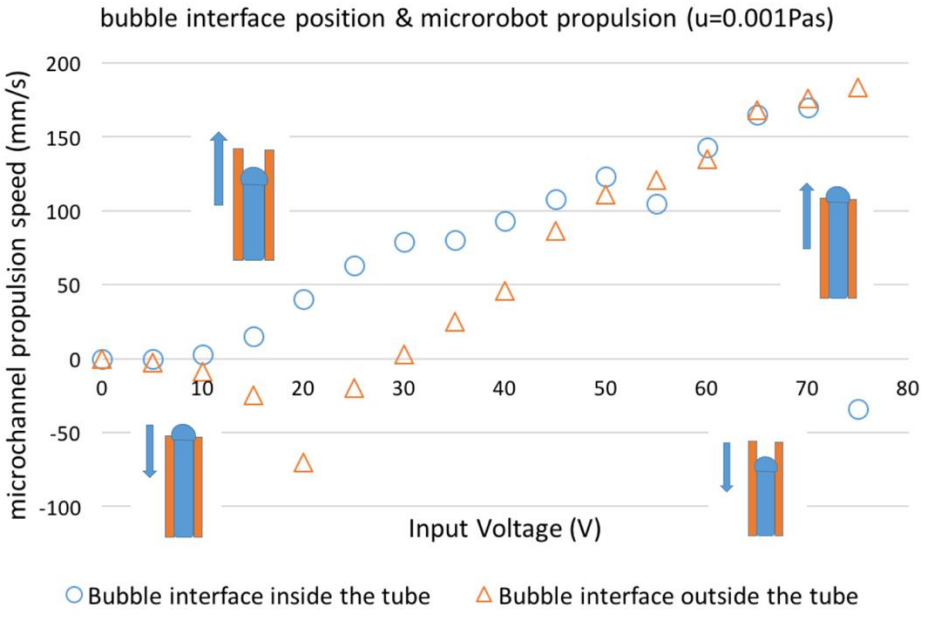

Figure 36. The relationship between stream speed and input voltage (u =0.001Pas)

2.4 METHOD TO IMPROVE THE SOUND TRANSMISSION

2.4.1 Experiment principle

During the blood testing I find out micro-swimmer move much slower than in water, so I decided to improve the sound transmission efficiency. The principle of the experiment is when ultrasonic wave transfer through the two materials at an oblique angle, which the materials have different a refractive index, there will be refracted waves generated. They follow Snell's Law:

$$\frac{sin\theta_1}{sin\theta_2} = \frac{v_1}{v_2} = \frac{\lambda_1}{\lambda_2} = \frac{n_2}{n_1} \tag{2-4}$$

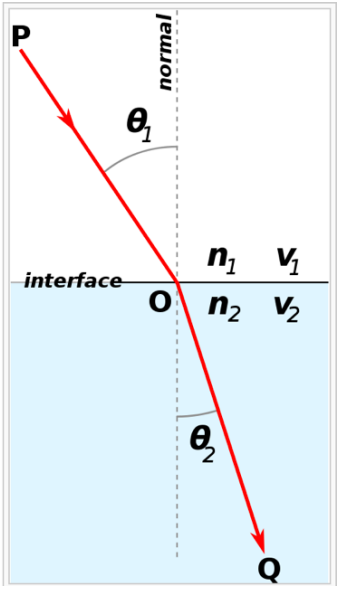

Figure 37. Snell's Law

Which θ is regarded as a boundary from the vertical angle measured. V is the speed of light/sound wave in each medium (SI units are meters per second, or *m/s*). λ is the wavelength of light in the respective medium and *n* is refractive index of each medium (unitless).

The reasons for I choose liquid lens are: structure of lens is not complicated and can change the focal length. The liquid lens has a wide range of application, and it have large potential for improvement, which can be applied later for the control in vivo micro-robot.

2.4.2 Experimental design and equipment build up

Liquid lens structure designing is shown below at figure 37, the elastic film is made by a cross-linkable polydimethyl siloxane (PDMS), which was provided by Dow Corning Corp. (Sylgard® 182). The cross-linkable PDMS was mixed as a viscous fluid and cross-linked at a w/w ratio of 10:1. By using rotating machine, I made the membrane, which thickness is 100 *um*. The production process for the liquid lens will be described below: Firstly, pick up PDMS solution 20g, using Karl Suss CT62 Spinner to produce membrane. Dripping photoresist on glass sheet and process in 1000 *r/min* rotation for 60*s*, so photoresist evenly coated on glass. Then drip the PDMS solution on a glass substrate. Select the spinner speed at 600 *r/min*, rotation for 60 *s*. Next, put the glass sheet into the oven in 60 ˚C, baking for about 30 *min*. After cooling for 4 hours, using acetone wash foam glass sheet, removing light plastic, letting glass sheet and PDMS membrane separation. Using alcohol rinse PDMS film, I can get a clean and complete PDMS film.

I chose metal flange as ring portion of the lens. The diameter of the upper surface is 40 *mm*, inner diameter is 26.20 *mm*. Between deformable PDMS membrane and the flange, I using optical glue (Dymax OP-29V, Dymanx Corp., Torrington CT) to adhesive them together. Under ultraviolet light irradiation is about 5 *min*, the metal flange can paste with PDMS membrane.

The PDMS sandwiched between Plexiglas and metal flanges, secured with bolts for reinforcement. Drilled two holes with 5mm in diameter in the side flanges, an input the liquid through one of it, exhaust gas from the other. A solid biconcave lens is attached in the bottom to maximize the use of space, so the focal length can be short enough. Then, I need to select liquid lens inside the lens. Sound waves will transmit through the liquid medium within the lens. When sound waves transmit through the intermediate compartment, then the reflection and refraction will be different. We need to select suitable liquid by compare sound intensity transmission coefficient:

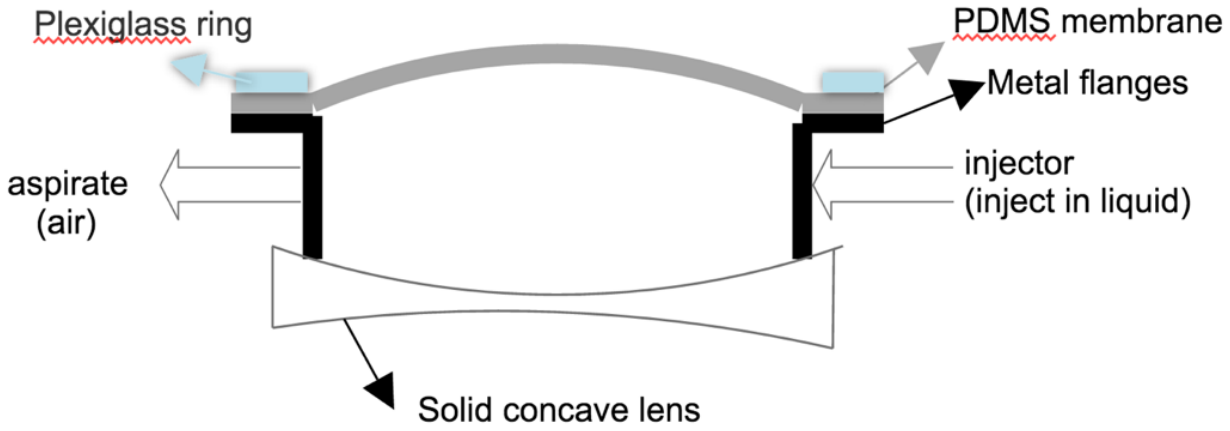

Figure 38. Structure of Lens

$$t_p = \frac{p_{ta}}{p_{ia}} = -\frac{1}{1 + \frac{1}{4}(R_{12} - R_{21})^2 sin^2 k_2 D} \tag{2-5}$$

I chose the cooking oil as an intermediate medium, because it is easy to get, and its density is close to the density of water, which will cause less attenuation. For method for liquid input, I used medical glass syringes direct injection liquid of liquid lens at first. Later I improved the inject method by using Harvard PHD 2000 to get more precise control.

Experimental platform structure is shown in figure 39. The tube will be placed in the bottom of the tank, so it is easily to be observed. The sound source is piezoelectric, which is attached on the top. The liquid lens, tube and sound source are in three-point line, and tube is immersed in the tank. Liquid lens us fixed by the holder (SUSS PH120 Manual ProbeHead) and a lens holder made by myself. It can be accurately moved in three dimensions. Microscope observe tube from the bottom. I measuring the vibration amplitude of the bubble in tube to determine the energy transmission efficiency.

First, I tested the bubble oscillation amplitude after liquid lens focus the acoustic wave. By changing the distance of the lens from tube in the z direction (vertical direction of paper consider as z direction). Firstly, I find the focal length, I try to change the lens position in the x, y direction (x direction, perpendicular out to the paper. y-axis the horizontal to paper). Observe amplitude changes. Figure 40 shows the change in the y direction. Figure 41 shows the change in the x direction. From the figure 40 we can see, in the central part of the liquid lens, we got the max value of the oscillation amplitude of the air bubbles, which is caused by acoustic liquid lens focusing sound field. At the position where bubble got maximum oscillate amplitude, the sound field is the strongest. So, the figure 41 description the acoustic liquid lens focusing effect.

So, I tested the liquid lens at the center of the focus line. By changing the input voltage, I test vibration of air bubbles, which can be seen from the figure 41, From the figure 42, by compare the bubble oscillation amplitude with/without liquid lens, we can see that the amplitude of the

bubble has been significantly improved, so we can get the conclusion that by using the liquid lens, we can focus the sound field, which can be used for improve the sound transmit efficiency

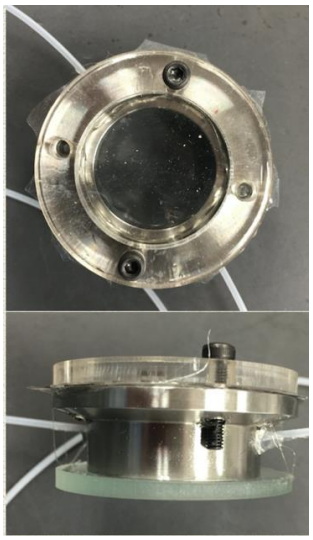

Figure 39. Top/side view of liquid lens

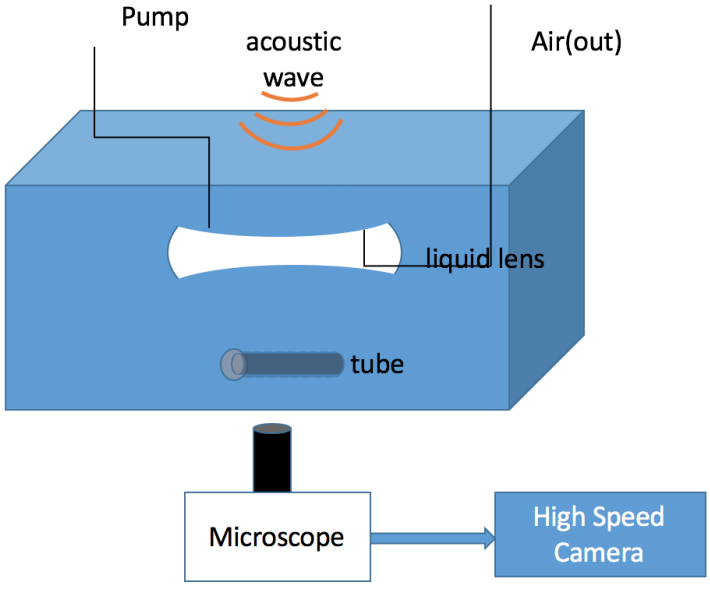

Figure 40. Experiment testing platform set up

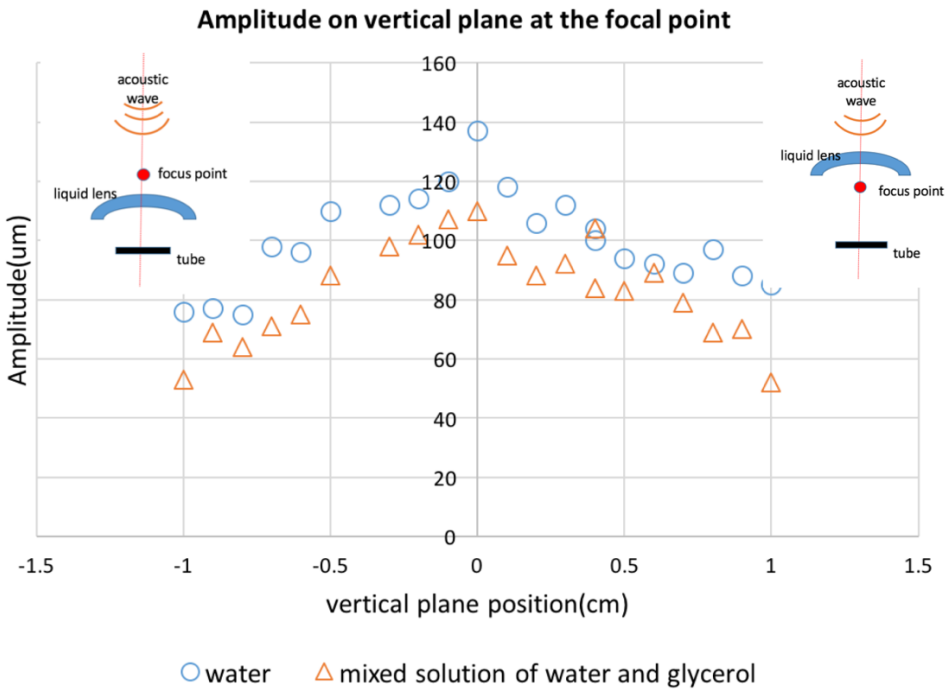

Figure 41. Experiment result for Amplitude on vertical plane at the focal point

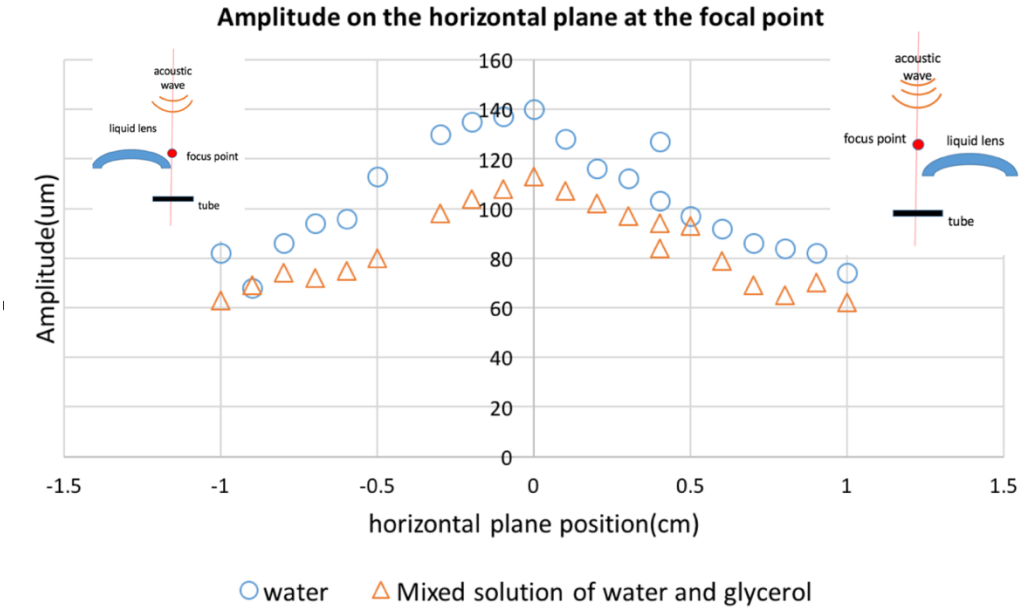

Figure 42. Experiment result for Amplitude on horizontal plane at the focal point

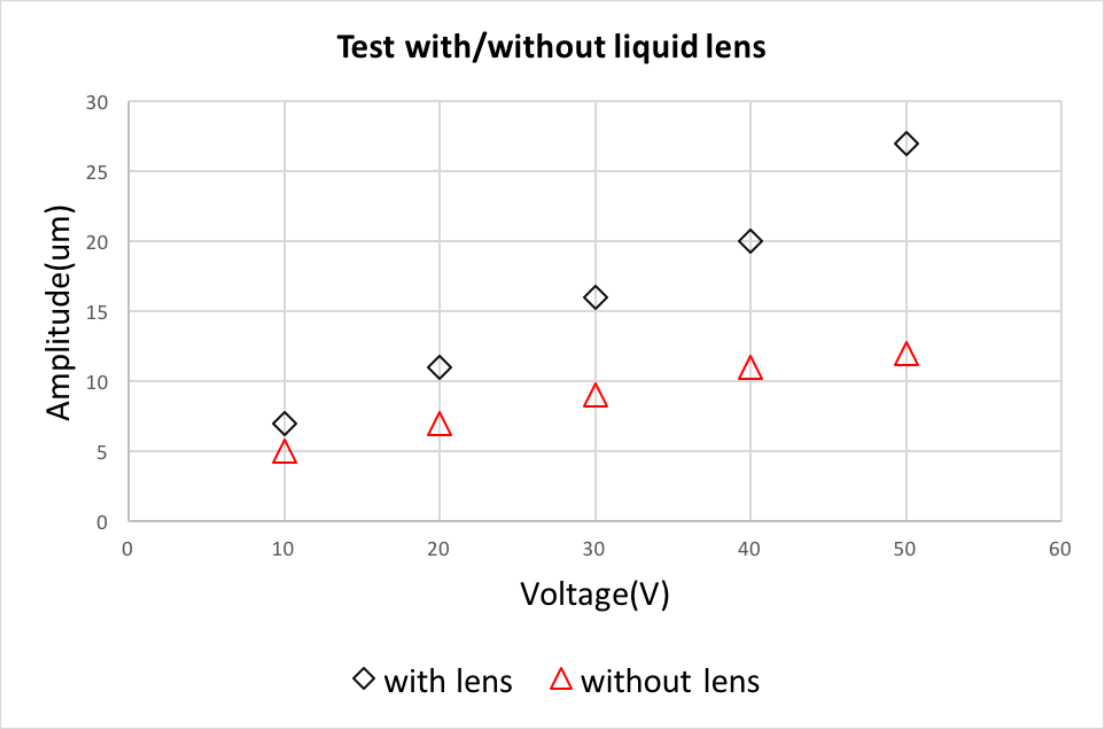

Figure 43. Experiment result for with/without liquid lens

3.0 FUTURE WORK

(1) Gas within the tube material selection

Because this kind of micro-swimmer move forward based on bubble-vibration. Eventually we hope that it can be applied to the human or animal body. In my experiments, I found out that the position of the bubble will vary in different situations, even the gas can overflow tube. Such a situation would occur in vivo biological impact. If the air inside the tube overflow within the blood vessel or tissue, and gas in the tube will adversely affect the living body. So, I want to test different types of gas, charged into the tube, dissolves in the blood, and test the affect to blood environment. I can also test different properties of the gas, the impact of the tube propulsion.

Here I plan to charge CO_2, oxygen in tube, these kind of gas can be taken away by blood or absorbed into the blood, reducing the impact on the biological environment. Jian Feng has been carried out using different materials made micro-swimmer, testing decomposition time in the blood. My plan is: find out experimental material can be absorbed or discharged by an organism, instead of being dissolved.

(2) Control the position of the bubble

Through the experiment in this thesis we can know. By changing the position of the bubble, I can make changes in the flow field around the tube. Apart from by applying the external sound field to vibrate bubble. By reading literature [92], We can guess, by changing the temperature and

light around the bubbles, we can control the growth of the bubble. For instance: using a laser directly irradiated on the tube containing bubble. To control the position of the bubble in the tube.

(3) Simulation Calculation of Flow Field around Bubble

In this thesis, I describe micro-swimmer have different movement phenomenon when bubbles in different positions, I also give the explanations of this phenomenon which were summarized from the experiment results. However, I did not give physical explanations on this phenomenon, I do not know what physical reason for this phenomenon, and I also can't give the specific physical parameters which will effect the direction of the micro-robot propulsion. Such as: the size/shape of the micro-robot, fluid velocity generated by bubble oscillation in micro-robots. I hope by using ANSYS calculations, I can describe the impact of the different positions of air bubble interface to the micro-swimmer propel direction. What's more, by computer simulation, I can know the streamline of the micro-fluid.

(4) Further Verification for Acoustic Lens

From the existing formula and we know that if we want to focus the light, the light wavelength is very important. From the existing formula I mentioned above, I just verified the sound waves transmit through different media, there will be refracted and focused. However, I did not verify the relationship between the vibration frequency and the lens curvature. So I can not fully determine, at acoustic frequencies of 3*kHz* (I use in the experiments), micro-swimmer movement is enhanced because of sound focusing. Other reasons, such as: With the addition of the lens, the acoustic transfer way changes, leading to the same result. In addition, the reproducibility of the experimental results is very low, so it is necessary to do more experiments to further control the

experimental variables, in this way I can make sure the lens can focus on low frequency sound waves.

REFERENCES

[1] J. V. Josepha, M. Aryab, and H. R. Patel, "Robotic surgery: the coming of a new era in surgical innovation," *Expert Rev. Anticancer Ther,* vol. 5, pp. 7-9, 2005.

[2] B. J. Nelson, I. K. Kaliakatsos, and J. J. Abbott, "Microrobots for Minimally Invasive Medicine," *Annu. Rev. Biomed. Eng,* vol. 12, pp. 55-85, 2010.

[3] P. Dario, M. C. Carrozza, A. Benvenuto, and A. Menciassi, "Menciassi A. 2000. Micro-systems in biomedical applications," *J. Micromech. Microeng,* vol. 10(2), pp. 235–44, 2000.

[4] M. J. Mack, "Minimally invasive and robotic surgery," *J. Am. Med. Assoc,* vol. 285(5), pp. 568–572, 2001.

[5] F. Tendick, S. S. Sastry, R. S. Fearing, and M. Cohn, "Applications of micromechatronics in minimally invasive surgery," *IEEE/ASME Trans. Mechatron,* vol. 3(1), pp. 34–42, 1998.

[6] G. Vince and C. Wilson, "The rise of the miniature medical robots," *New Sci,* vol. 204, pp. 50–53, 2009.

[7] M. Sitti, "Voyage of the microbots," *Nature,* vol. 458, pp. 1121-1122, 2009.

[8] L. Rubinstein, "A Practical Nanorobot for Treatment of Various Medical Problems," in *In Proceedings of the 8th Foresight Conference on Molecular Nanotechnology*, Bethesda, MD, USA.

[9] G. Vince and C. Wilson, "The rise of the miniature medical robots," *New Sci,* vol. 204, pp. 50-53, 2009.

[10] M. Sitti, "Voyage of the microbots," *Nature,* vol. 458, pp. 1121–1122, 2009.

[11] L. Rubinstein, "A Practical Nanorobot for Treatment of Various Medical Problems," in *In Proceedings of the 8th Foresight Conference on Molecular Nanotechnology*, Bethesda, MD, USA, 2000.

[12] G. Dogangil, O. Ergeneman, J. J. Abbott, S. Pane, H. Hall, S. Muntwyler*, et al.*, "Towardtargetedretinaldrugdelivery with wireless magnetic microrobots," in *Proc. IEEE/RSJ Int. Conf. Intell. Robots Syst*, Nice, Fr, 2008, pp. 1921–1926.

[13] M. Sendoh, K. Ishiyama, K. I. Arai, M. Jojo, F. Sato, and H. Matsuki, "Fabricationofmagneticmicromachine for local hyperthermia," *IEEE Trans. Magn,* vol. 38, pp. 3359–3361, 2002.

[14] F. Sato, M. Jojo, H. Matsuki, T. Sato, M. Sendoh, K. Ishiyama*, et al.*, "The operation of a magnetic micromachine for hyperthermia and its exothermic characteristic," *IEEE Trans. Magn,* vol. 38, pp. 3362-3364, 2002.

[15] S. Byun, J.-M. Lim, S.-J. Paik, A. Lee, K.-i. Koo, S. Park*, et al.*, "Barbed micro-spikes for micro-scale biopsy," *J.Micromech. Microeng,* vol. 15, pp. 1279–1284, 2005.

[16] A. C. Jones, B. Milthorpe, H. Averdunk, A. Limaye, T. J. Senden, A. Sakellariou*, et al.*, "Analysis of 3D bone ingrowth into polymer scaffolds via micro-computed tomography imaging," *Biomaterials,* vol. 25, pp. 4947–4954, 2004.

[17] J. Feng and S. K. Cho, "Mini and Micro Propulsion for Medical Swimmers," *Micromachines,* vol. 5, pp. 97-113, 2014.

[18] E. M. Purcell, "Life at Low Reynolds Number," *Am. J. Phys,* vol. 45, pp. 3-11, 1977.

[19] J. Happel and H. Brenner, *Low Reynolds Number Hydrodynamics*. New York: Martinus Nijhoff Publishers, 1983.

[20] S. Kim and S. J.Karrila, *Microhydrodynamics: Principles and Selected Applications*. Mineola, New York: Dover Publications, 2005.

[21] L. G. Leal, *Advanced Transport Phenomena: Fluid Mechanics and Convective Transport Processes*, 2010.

[22] J. Hinch, *Hydrodynamics at Low Reynolds Numbers: A Brief and Elementary Introduction*: Springer Netherlands, 1988.

[23] P. C, *Theoretical and Computational Fluid Dynamics*: Oxford: Oxford University Press, 2000.

[24] S. Vogel, *Comparative Biomechanics: Life's Physical World* Princeton, NJ: Princeton University Press, 2003.

[25] R. Dudley, *TheBiomechanicsofInsectFlight: Form, Function, Evolution*. Princeton, NJ: Princeton University Press, 2002.

[26] D. E. Alexander, *Nature's Flyers: Birds, Insects, and the Biomechanics of Flight* Baltimore, MD: The Johns Hopkins University Press, 2002.

[27] S. Vogel, *Life in Moving Fluids*, Second edition ed. Princeton,NJ: Princeton University Press, 1996.

[28] C. Ellington, *The Aerodynamics of Hovering Insect Flight* vol. 305. London: The Royal Society, 1984.

[29] S. Childress, *Mechanics of Swimming and Flying*. Cambridge: Cambridge University Press, 1981.

[30] R. J. Dijkink, J. P. v. d. Dennen, C. D. Ohl, and A. Prosperetti, "The 'acoustic scallop': a bubble-poweredactuator," *J. Micromech. Microeng,* vol. 16, pp. 1653–1659, 2006.

[31] J. Feng and S. K. Cho, "Micro Propulsion in Liquid by Oscillating Bubbles," in *IEEE 26th International Conference on Micro Electro Mechanical System*, Taipei, Taiwan, January 2013, pp. 63–66.

[32] J. E. Avron and O. Raz, "Ageometrictheoryofswimming: Purcell's swimmer and its symmetrized cousin," *New J. Phys,* vol. 10, 2008.

[33] D. Tam and A. E. Hosoi, *Phys. Rev. Lett,* vol. 98, 2007.

[34] A. Najafi and R. Golestanian, "Simple swimmer at low Reynolds number: Three linked spheres," *Phys.Rev.E,* vol. 69, 2004.

[35] R. Dreyfus, J. Baudry, and H. A. Stone, "Purcell's "rotator": mechanical rotation at low Reynolds number," *Eur. Phys. J. B,* vol. 47, pp. 161–164, 2005.

[36] A. Najafi and R. Golestanian, "Propulsion at low Reynolds number," *J. Phys.: Condens. Matter,* vol. 17, pp. 203-208, 2005.

[37] R. Golestanian and A. Ajdari, "Analytic results for the three-sphere swimmer at low Reynolds number," *Phys. Rev. E* vol. 77, 2008.

[38] R. Golestanian, "Three spherelow Reynolds number swimmer with a cargo container," *Eur. Phys. J. E,* vol. 25, pp. 1-4, 2008.

[39] J. E. Avron and K. K. O, "Pushmepullyou: an efficient micro-swimmer " *New J. Phys,* vol. 7, p. 234, 2005.

[40] E. Lauga and T. R. Powers, "The hydrodynamics of swimming microorganisms," *Rep. Prog. Phys,* vol. 72, 2009.

[41] T. Honda, K. I. Arai, and K. Ishiyama, "Micro swimming mechanisms propelled by external magnetic fields," *IEEE Trans. Magn,* vol. 9, pp. 5085–5087, 1996.

[42] A. Ghosh and P. Fischer, "Controlled propulsion of artificial magnetic nanostructured propellers," *Nano Lett,* vol. 9, 2009.

[43] L. Zhang, J. J. Abbott, L. Dong, B. E. Kratochvil, D. Bell, and B. J. Nelson, "Artificial bacterial flagella: fabrication and magnetic control," *Appl. Phys. Lett,* vol. 94, 2009.

[44] B. Behkam and M. Sitti, "Design methodology for biomimetic propulsion of miniature swimming robots," *ASME J. Dyn. Syst. Meas. Control,* vol. 128, pp. 36–43, 2006.

[45] G. Kósa, P. Jakab, F. Jólesz, and N. Hata, "Swimming capsule endoscope using static and RF magnetic field of MRI for propulsion," in *Proc. IEEE Int. Conf. Robot. Autom.*, Pasadena, Calif., 2008, pp. 2922–2927.

[46] J. R. Howse, R. A. L. Jones, A. J. Ryan, T. Gough, R. Vafabakhsh, and R. Golestanian, "Self-motile colloidal particles: From directed propulsion to random walk," *Phys. Rev. Lett,* vol. 99, 2007.

[47] J. G. Gibbs and Y.-P. Zhao, "Autonomously motile catalytic nanomotors by bubble propulsion," *Appl. Phys. Lett,* vol. 94, 2009.

[48] J. Vicario, R. Eelkema, W. R. Browne, A. Meetsma, R. M. L. Crois, and B. L. Feringa, "Fuelling autonomous movement by a surface bound synthetic manganese catalase," *Chem. Commun,* pp. 3936–3938, 2005.

[49] A. A. Solovev, Y. Mei, E. B. Ureña, G. Huang, and O. G. Schmidt, "Catalytic microtubular jet engines self-propelled by accumulated gas bubbles," *Small* vol. 5, pp. 1688–1692, 2009.

[50] W. Gao, A. Uygun, and J. Wang, "Hydrogen-bubble-propelled zinc-based microrockets in strongly acidic media," *J. Am. Chem. Soc,* vol. 134, pp. 897–900, 2012.

[51] P. Hanggi and F. Marchesoni, "Artificial Brownian motors: Controlling transport on the nanoscale," *Rev. Mod. Phys,* vol. 81, pp. 387-442, 2009.

[52] I. Buttinoni, G. Volpe, F. Kümmel, G. Volpe, and C. Bechinger, "Active Brownian motion tunable by light," *J. Phys. Condens. Matter,* vol. 24, 2012.

[53] R. Golestanian, T. B. Liverpool, and A. Ajdari, "Designing phoretic micro- and nano-swimmers," *New J. Phys,* vol. 9, p. 126, 2007.

[54] H.-R. Jiang, N. Yoshinaga, and M. Sano, "Active motion of a Janus particle by self-thermophoresis in a defocused laser beam," *Phys. Rev. Lett,* 2010.

[55] D. D.Joseph, "Instability of the flow of two immiscible liquids with different viscosities in pipe," *J. Fluid Mech,* vol. 141, pp. 309-317, 1984.

[56] **C.-M. Ho** and **Y.-C. Tai**, "Micro-Eelectro-Mechanical-Systems (MEMS) and Fluid Flows," *Annu. Rev. Fluid Mech,* pp. 579–612, 1998.

[57] Y. Renardy, "Instabilities in Steady Flows of Two Fluids," *J. of Math,* vol. 8, pp. 455-477, 1988.

[58] H. C. Brinkman, "A Calculation of the Viscous Force Exerted by a Flowing Fluid on a Dense Swaem of Particles," *Appl. Sci. Res,* vol. A1, pp. 27-34, 1947.

[59] M. Minnaer, "On musical air bubbles and sound of running water," *Philosophical Magazine,* vol. 16, pp. 235-248, 1993.

[60] H. N. Oğuz and A. Prosperetti, "The natural frequency of oscillation of gas bubbles in tubes," *J. Acoust. Soc. Am.,* vol. 103, pp. 3301-3308.

[61] H. Levine and J. Schwinger, "On the Radiation of Sound from an Unfianged Circular Pipe," *Physical Review,* vol. 73, pp. 383-406, 1948.

[62] J. Feng, J. Yuan, and S. K. Cho, "Micropropulsion by an acoustic bubble for navigating microfluidic spaces," *Lab Chip,* vol. 15, pp. 1554-1562, 2015.

[63] Cutnell, John, Johnson, and Kenneth, *Physics*, Fourth Edition ed., 1998.

[64] Benson and Katherine, *MCAT Review*: Emory University, 1999.

[65] E. Margolis, J.Gurevitch, and E. Hasson, *Blood*: Funk and Wagnalls Encyclopedia., 1985.

[66] Hinghofer-Szalkay, H.G., Greenleaf, and J.E., "Continuous monitoring of blood volume changes in humans," *Journal of Applied Physiology,* vol. 63, pp. 1003-1007, 1987.

[67] N. Ageyama, "Specific Gravity of Whole Blood in Cynomolgus Monkeys, Squirrel Monkeys, and Tamarins," *Contemporary Topics in Laboratory Animal Science,* vol. 40, 2001.

[68] H. RE and C. YI, *Advancing Medicine with Food and Nutrients*, Second Edition ed.: CRC Press, 2012.

[69] G. Elert, *Viscosity. The Physics Hypertextbook*.

[70] P. Marmottant and S. Hilgenfeldt, "Controlled vesicle deformation and lysis by single oscillating bubbles," *Nature,* vol. 423, pp. 153-156, 2003.

[71] C. J, M. R, L. P, T. P, O. A, P.-D. K*, et al.*, "Cavitation microstreaming and stress fields created by microbubbles," *j.ultras,* vol. 50(2), pp. 273-279, 2010.

[72] J. Collis, R. Manasseh, P. Liovic, P. Tho, A. Ooi, K. Petkovic-Duran*, et al.*, "Cavitation microstreaming and material transport around microbubbles," *J. phpro,* vol. 3, pp. 427–432, 2010.

[73] R. H. Liu, R. Lenigk, R. L. Druyor-Sanchez, J. Yang, and P. Grodzinski†, "Hybridization Enhancement Using Cavitation Microstreaming," *Anal. Chem,* vol. 75, pp. 1911-1917, 2003.

[74] S. A. Elder, "Cavitation Microstreaming," *Acoust. Soc. Am,* vol. 29, pp. 54-64, 1958.

[75] mashephe1. (2011). *Acoustic Lenses*. Available: https://www.youtube.com/watch?v=KnjzJkBboc4

[76] H. Ren, D. Fox, P. A. Anderson, B. Wu, and S.-T. Wu, "Tunable-focus liquid lens controlled using a servo motor," *Opt. Express,* vol. 14, pp. 8031-8036, 2006.

[77] H. Ren and S.-T. Wu, "Variable-focus liquid lens " *Opt. Express,* vol. 15, pp. 5931-5936, 2007.

[78] S. W. Lee and S. S. Lee, "Focal tunable liquid lens integrated with an electromagnetic actuator," *Appl. Phys. Lett. 9,* vol. 90, pp. 121129 1-3, 2007.

[79] C.-C. Cheng and J. A. Yeh, "Dielectrically actuated liquid lens " *Opt. Express,* vol. 15, pp. 7140-7145, 2007.

[80] H. Oku and M. Ishikawa, "High-speed liquid lens with 2 ms response and 80.3 nm root-mean-square wavefront error," *Appl. Phys. Lett.,* vol. 94, p. 221108, 2009.

[81] S. Kuiper and B. H. W. Hendriks, "Variable-focus liquid lens for miniature cameras," *Appl. Phys. Lett.,* vol. 85, pp. 1128-1130, 2004.

[82] M. Vallet and B. Berge, "Electrowetting of water and aqueous solutions on poly(ethylene terephthalate) insulating films," *Polymer Vol.,* vol. 37, pp. 2465-2470, 1996.

[83] T. Krupenkin, S. Yang, and P. Mach, "Tunable liquid microlens," *Appl. Phys. Lett.,* vol. 82, pp. 316-318, 2003.

[84] J. Chen, W. Wang, J. Fang, and K. Varahramyan, "Variable-focusing microlens with microfluidic chip," *J. Micromech. Microeng.,* vol. 14, pp. 675–680, 2004.

[85] K.-H. Jeong, G. L. Liu, N. Chronis, and L. P. Lee, "Tunable microdoublet lens array " *Opt. Express,* vol. 12, pp. 2494-2500, 2004.

[86] D.-Y. Zhang, V. Lien, Y. Berdichevsky, J. Choi, and Y.-H. Lo, "Fluidic adaptive lens with high focal length tunability," *Appl. Phys. Lett.,* vol. 82, pp. 3171-3172, 2003.

[87] G. Beadie, M. L. Sandrock, M. J. Wiggins, R. S. Lepkowicz, J. S. Shirk, M. Ponting*, et al.*, "Tunable polymer lens," *Opt. Express,* vol. 16, pp. 11847-11857, 2008.

[88] N.-S. Cheng, "Formula for Viscosity of Glycerol-Water Mixture " *Ind. Eng. Chem. Res,* vol. 47, pp. 3285-3288, 2008.

[89] . *Viscosity*. Available: http://www.met.reading.ac.uk/~sws04cdw/viscosity_calc.html

[90] . Available: https://en.wikipedia.org/wiki/Blood_plasma

[91] (2004). *Density of Blood*. Available: http://hypertextbook.com/facts/2004/MichaelShmukler.shtml

[92] D. Ahmed, M. Lu, A. Nourhani, P. E. Lammert, Z. Stratton, H. S. Muddana*, et al.*, "Selectively manipulable acoustic-powered microswimmers," *Sci. Rep.,* vol. 5, 2015.